THE REMOVAL OF NITROGEN-16 FROM REACTOR COOLING WATER

by

Ernest James Coppola

THE REMOVAL OF NITROGEN-16 FROM REACTOR COOLING WATER

by

ERNEST JAMES COPPOLA

S.B., United States Naval Academy

(1964)

SUBMITTED IN PARTIAL FULFILLMENT

OF THE REQUIREMENTS FOR DEGREES

OF NAVAL ENGINEER AND MASTER OF SCIENCE

at the

MASSACHUSETTS INSTITUTE OF TECHNOLOGY

May, 1969

THE REMOVAL OF NITROGEN-16 FROM REACTOR COOLING WATER

by

ERNEST JAMES COPPOLA

Submitted to the Department of Naval Architecture and Marine Engineering on May 24, 1969 in partial fulfillment of the requirements for the degree of Naval Engineer; and to the Department of Nuclear Engineering on May 24, 1969 in partial fulfillment of the requirement for the degree of Master of Science.

ABSTRACT

A formidable problem that must presently be contended with in all reactors using water as a coolant or moderator is the production of nitrogen-16 activity due to the O^{16} (n,p) N^{16} reaction of fast neutrons with oxygen from the water molecule. N-16 is radioactive and decays back to O-16 through beta emission, followed immediately by a 6.13 MeV gamma ray in 69% of all decays. This means that the primary cooling loop must be heavily shielded, and on-line maintenance severely curtailed.

In the present work, a previously constructed closed loop system was evaluated and improved to permit the production and study of N-16 water chemistry at the MIT reactor. It was found that the N-16 was produced in predominately ionic form, 40% being removed by cation resin and 80% by anion resin. Dissolved gases, including air, nitrogen, helium, hydrogen and oxygen were shown to have no effect on the ion distribution produced by the facility. Zirconium-dioxide was studied as a potential filter medium capable of withstanding PWR operating temperatures, and was found to remove as much as 44% of the N-16 in a single pass.

Thesis Supervisor: Michael J. Driscoll
Title: Assistant Professor of Nuclear Engineering

ACKNOWLEDGEMENTS

I would like first of all to acknowledge my advisor, Professor Michael Driscoll, who provided sound guidance throughout, and who deserves much credit for the success of this work.

The entire staff of the reactor building was very helpful, almost every individual providing some assistance along the way. Special thanks go to Al Supple who provided help in all phases of the experimental work. The final acknowledgement is well deserved by Miss Diane Mountain, who so expertly typed the final report.

TABLE OF CONTENTS

LIST OF FIGURES

LIST OF TABLES

CHAPTER I

INTRODUCTION

1.1 Background

The problem of nitrogen-16 activation in reactor cooling water is extensively discussed in Ref. 1. In summary, N-16 is present as a result of the O^{16} (n,p) N^{16} reaction of fast neutrons with oxygen from the water molecule. The threshold for this reaction is 10.3 MeV and the cross section increases to a maximum of about 100 mb at 13.5 MeV before falling off at higher energies (1). N-16 decays by beta emission to O-16, with a half-life of 7.1 seconds, and the excited oxygen atom returns almost immediately to its ground state by gamma emission, including a 6.13 MeV gamma ray in 69% of the decays. Figure 1.1 shows the decay scheme of N-16 (2).

There are other activities produced in reactor cooling water, but N-16 is by far the most important, as demonstrated by Table 1.1, which shows typical activities of various nuclides found in a PWR coolant.

The result of this water-borne N-16 activity is that the primary cooling loop must be heavily shielded, and that virtually no maintenance may be performed without a reactor shutdown - a costly proposition for a power reactor. These problems are of even greater magnitude for a small shipboard power reactor, where weight and space limitations are severe. The removal of some or all of the N-16 activity from the cooling

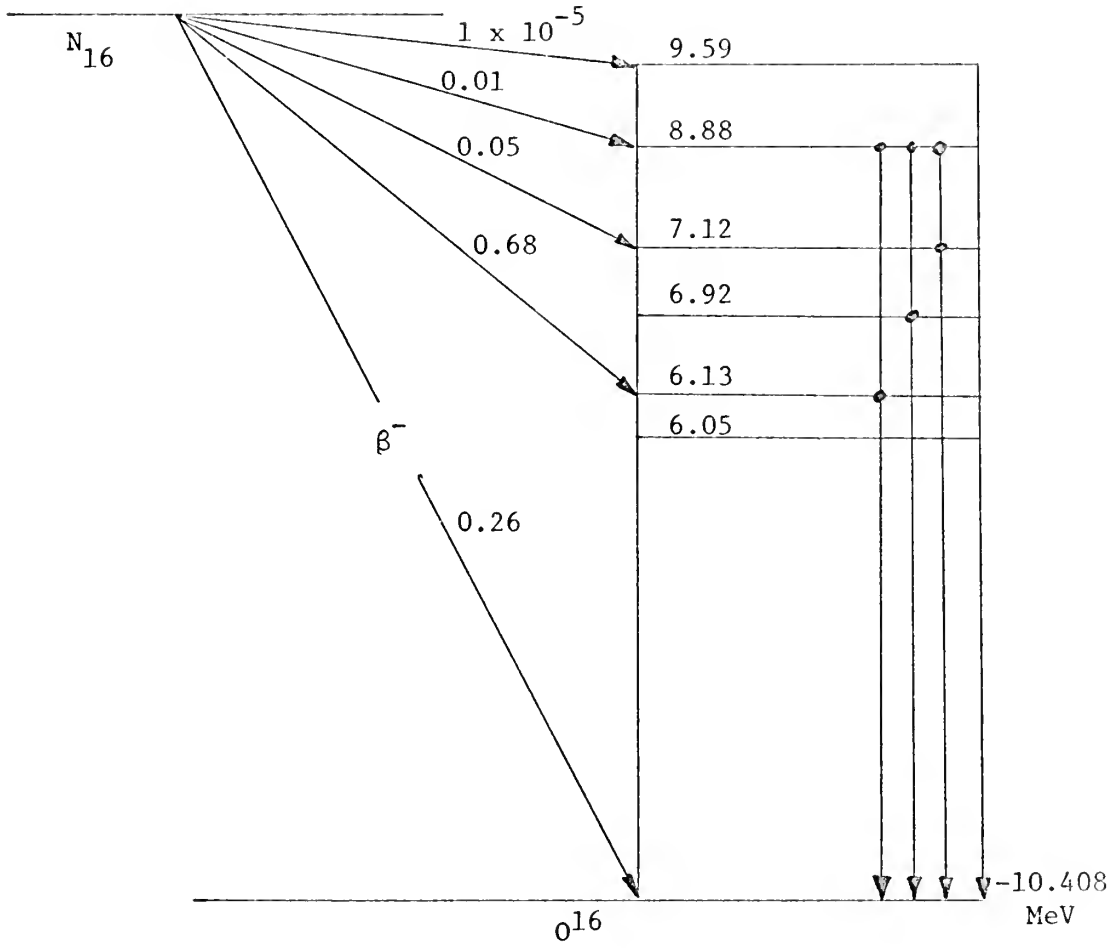

Figure 1.1

Decay Scheme of N-16

(adopted from Ref. 2)

Nuclide	Source	Activity
N^{16}	O^{16}	100 μ ci/ml
N^{17}	O^{17}, O^{18}	2.2×10^{-2} μ ci/ml
F^{18}	O^{18}	4×10^{-2} μ ci/ml
K^{38}	?	5×10^{-2} μ ci/ml
All Others	Various	each $\leq 4 \times 10^{-2}$ μ ci/ml

Table 1.1

Typical Activities in PWR Coolant

(adopted from Ref. 1)

water of this type of shipboard reactor would allow a decrease in ship size and resultant increase in speed, since the total reactor plant shielding could be reduced in weight by about one-half. In addition, the ship would be more operationally flexible because on-line maintenance of the primary cooling loop would then be possible.

The above effects represent a savings in cost and an increase in reliability. For the shipboard reactor system the increase in reliability and operational flexibility would predominate. For the shore-based power reactor, however, the predominant feature would be the potential savings in cost.

For the above reason it appeared that there is a real incentive to investigate the water chemistry of N-16 and seek an effective method for its removal.

1.2 N-16 Half-Life

Several values for the N-16 half-life have been reported in the literature (7.35, 7.31, 7.14 sec.); 7.35 sec. being the most common. It thus appears that the problem of competing activities has not been entirely solved. Much of the work previously done on N-16 detection involved only low level descrimination and it is believed that bremsstrahlung from O-19 (reported half-life of 2.3 sec.) might have increased the indicated "N-16" half-life. S. A. Scott (Technion - Israel) and A. Notea (Israel AEC) recently undertook an experiment at IRR-1 to accurately determine the half-life of N-16 (3). A 3.75 MeV energy discrimination level was employed and the data plotted and curve

fitted by "least squares" with exponential series having constant exponents. The analysis yielded two distinct curves showing half-lives of 29 and 7.1 sec., indicating that previously reported half-lives of O-19 and N-16 had been mutually biased. Thus 7.1 sec. will be used as the half-life of N-16 in all calculations in this report.

1.3 N-16 Removal

Several experimenters have previously studied N-16 and its removal from water, notably Driscoll (4), Forbes (5), Mestemaker (1), and the present author (6) at MIT. Driscoll and Forbes removed small amounts of N-16 activity by filtration with activated charcoal. Mestemaker constructed the present N-16 facility and achieved 15% removal with activated charcoal and 75% removal with H-OH ion exchange resin, the latter indicating that water-borne N-16 is predominately ionic in form. The present author in a 13.71 course project then modified Mestemaker's N-16 facility and achieved removals of 90% with OH^- resin and 43% with H^+ resin. This same facility, with further modifications, was used to carry out the experiments to be described in this report.

1.4 Suitable Filter Material

Although ion exchange resins have removed up to 90% of the activity produced by the N-16 facility, these materials are unsuitable for use in a PWR because of their chemical instability at high temperatures. Several inorganic materials, able to withstand PWR temperatures, show

promise as possible N-16 filtering agents. They will be discussed in detail in Chapter IV.

1.5 Objectives of Present Work

The objectives of this thesis are:

1.) To determine the specific characteristics of the N-16 facility in order to account for any built-in bias in the data obtained.

2.) To confirm previous evidence of N-16 removal, and more accurately define the effect of cover gas on the N-16 system.

3.) To seek and test materials, such as inorganic filtering agents, that will remove significant amounts of N-16 activity and still be chemically stable at PWR temperatures.

The next three chapters deal with each of these objectives in turn.

CHAPTER II

EXPERIMENTAL APPARATUS

2.1 Description of Apparatus

The N-16 facility used in this experiment was designed and constructed by R. Mestemaker in the winter of 1968, and subsequently modified by the author. Detailed descriptions of the original design may be found in Refs. 1 and 6. In short, the N-16 loop consists of two major sections, the in-pile section and the out-of-pile section.

The in-pile section consists of six 2% enriched uranium fuel rods clustered around an aluminum U-tube through which the water to be irradiated flows. This assembly is inserted into a 2-inch diameter aluminum tubular housing, which is in turn inserted into the MITR Hohlraum.

The out-of-pile section consists of a portable cart holding the electronics, detector, shielding, filters, pump, gas bottles, purge tank, and aluminum tubing to complete the water flow path. A schematic of the system layout is shown in Figure 2.1. With a few exceptions the design is the same as constructed by Mestemaker.

Figure 2.2, a picture of the front of the cart, shows the purge tank, pump, pressure gage, flow meter, and filter bank. Several small equipment alterations will be described subsequently.

The detector employs a sodium iodide scintillator plus photomultiplier tube to detect the 6.13 MeV gamma given off by the N-16

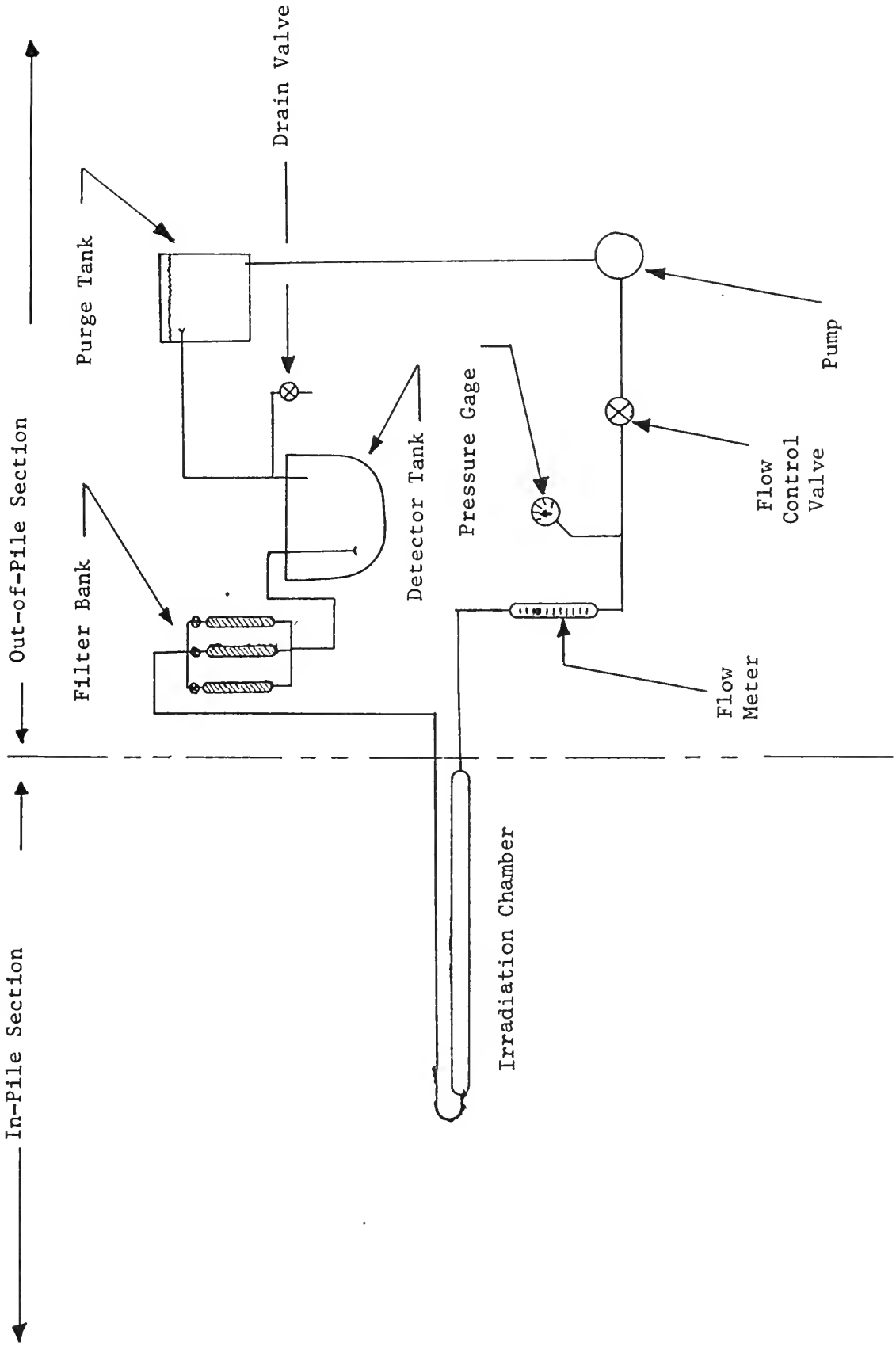

Figure 2.1
Schematic of MIT N-16 Facility

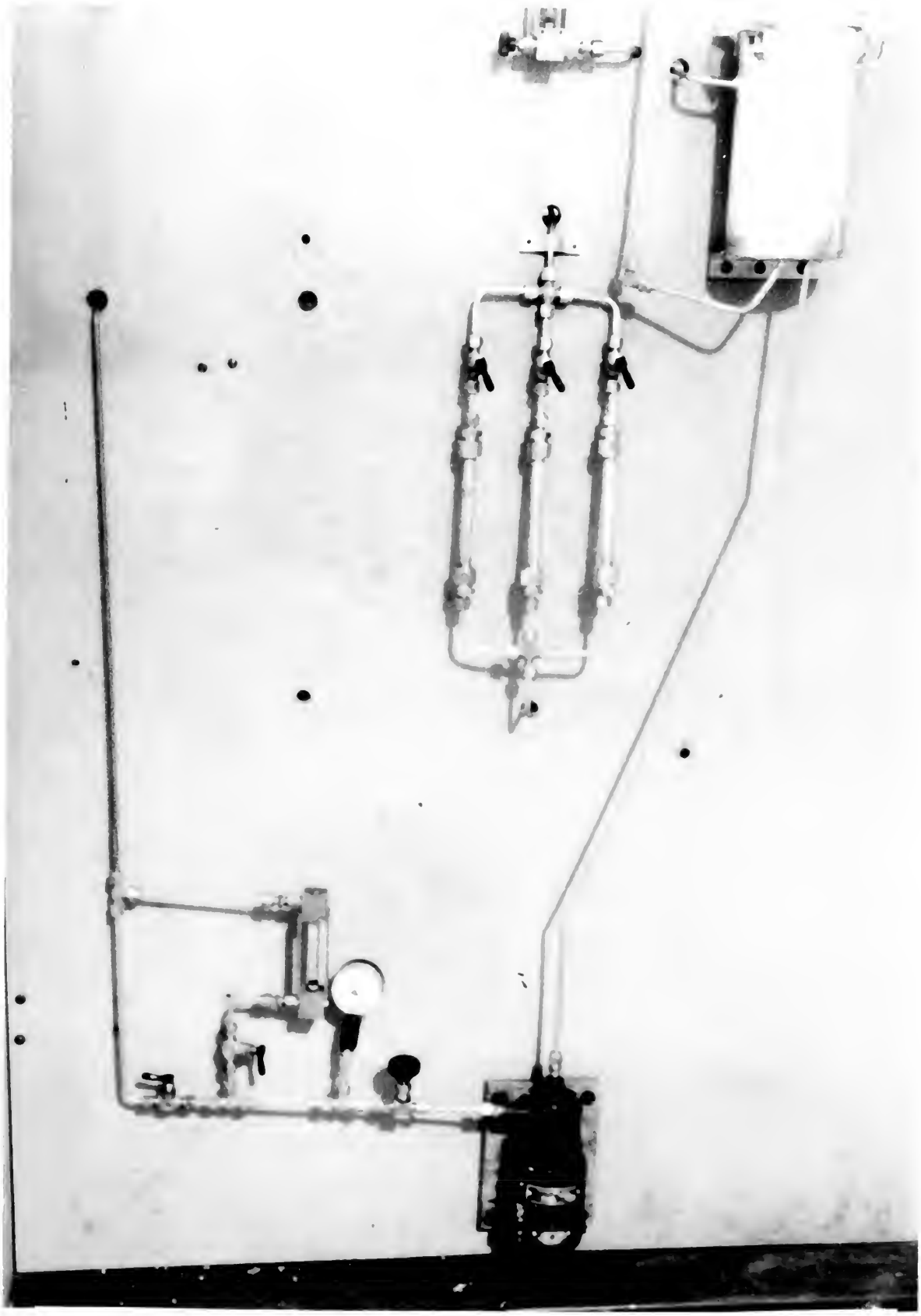

Fig. 2.2 Flow Components on Front of N-16 Cart

activity in the detector tank. A schematic of the counting electronics is shown in Fig. 2.3.

2.2 Disadvantage of Present System

The main disadvantage of the present detection system is that the high N-16 background from the MITR requires heavy and bulky shielding of the detector on the N-16 cart in order to obtain reasonable signal to noise ratios. It is estimated that the detector shielding alone weighs about 1100 pounds. Thus the N-16 cart, while portable, is difficult to move about. For that reason, two alternative detection systems (N-17 neutron detector and Cerenkov detector) were investigated by R. Fay in conjunction with the author. These are described briefly in Appendix A. Since neither proved suitable they will not be discussed further here.

2.3 Previous Work Using the MIT N-16 Loop

R. Mestemaker, after completing construction of the N-16 loop in the winter of 1968, demonstrated its successful operation in producing N-16 activity, but did not carry out any studies on N-16 itself. The loop was modified by the author and used to test N-16 pickup of various materials during the summer of 1968. The details of the tests may be found in Ref. 6; but briefly, they consisted of:

1,) Measurement of N-16 activity as a function of flow rate. This measurement was made by passing the water through the center filter of the filter bank. This filter was filled with glass beads,

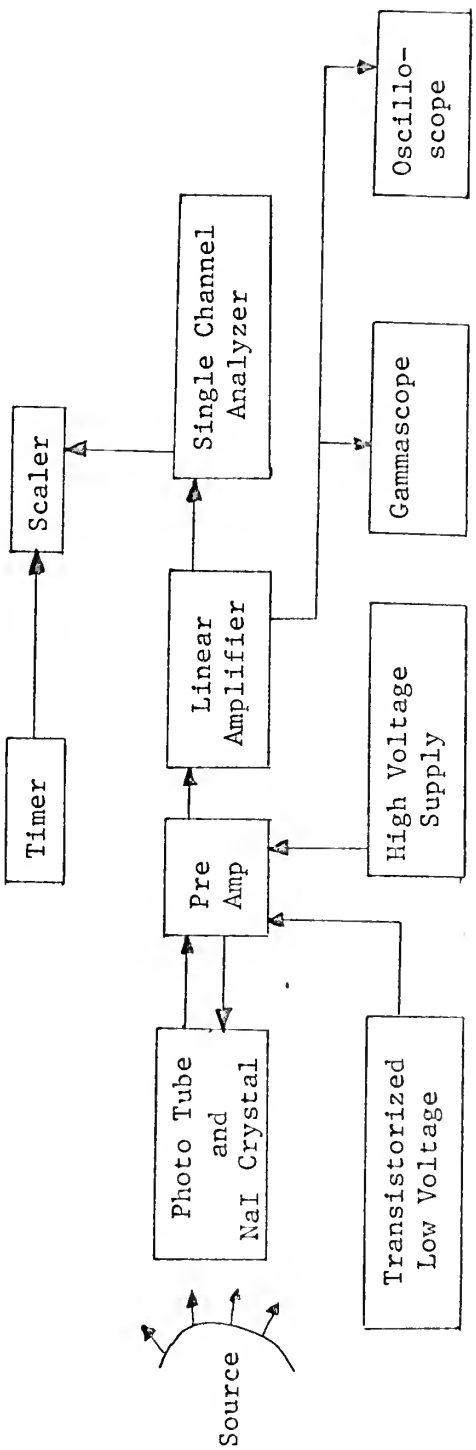

Figure 2.3

Schematic of Counting Electronics

which do not remove N-16 from the water, and served as a bench-mark condition with which to compare all other filter materials. The beads are present merely to fill the volume of the central filter tube to approximately the same degree as the test materials in the outer tubes.

2.) Measurement of N-16 pickup by both H^+ and OH^- ion exchange resins and by activated charcoal.

3.) A repeat of (2) above with nitrogen cover gas, and then with helium cover gas.

4.) A repeat of (2) above after adding ammonium hydroxide to the water.

5.) A repeat of (2) above after adding nitric acid to the water.

Briefly, the results of these tests were:

1.) N-16 activity increased monotonically with flow rate up to a nominal flowmeter reading of 10 gallons per hour, the maximum achievable flow rate for the present system. As will be discussed later, the actual flow rate was found to be 7.8 GPH when the flow meter was accurately calibrated.

2.) N-16 activity was removed by the ion exchange resins: approximately 40% by the H^+ resin and 90% by the OH^- resin.

3.) A definite change in resin removal fraction was noted after the gas purges, indicating, what was felt to be at the time, a possible alteration of the N-16 chemical distribution.

4.) An apparent saturation of the resins by the NH_4^+ and NO_3^- ions was noted, as indicated by drastically reduced N-16 pickup.

The quantitative results of these tests will not be discussed further because additional work with the loop suggested that a careful grooming of the equipment and the elimination of all possible sources of bias should be carried out before any further extensive test program.

2.4 Comparison of Theoretical and Experimental Activity Vs Flow Rate

In Ref. 1, Mestmaker calculated that N-16 activity, as indicated by count rate, should peak at a flow rate of about 8 GPH. Table 2.1, showing activity vs. flow rate, indicates that activity is still increasing rapidly at 8 GPH. It was therefore decided that the first step in determining loop bias was to resolve this inconsistency.

The detector count rate is proportional to the steady state activity in the detector chamber, the detector's efficiency being the constant of proportionality. This activity will depend on the concentration of N-16 in the effluent from the in-pile irradiation chamber, the amount of decay that occurs before reaching the detector chamber, and the amount of activity that passes out of the detector chamber with the effluent water.

The formulas for calculation of the relative N-16 activity in the detector chamber are derived in Appendix B. If, in the detector chamber, perfect mixing occurs, the decay rate in the chamber is given by:

Table 2.1

Counts Attributable to N-16 Activity*

(Counting Time = 50 Sec.)

Flow Rate	Counts
6.2 GPH	20,908
5.4	17,021
4.7	13,521
3.9	10,557
3.1	5,698
2.3	3,093

* gross count rate less background; (background measured with facility in place at zero flow.)

$$DR\ mixed = \underbrace{A_0(1 - e^{-\frac{\lambda V_1}{R}})}_{\text{Irradiation Chamber}} \underbrace{(e^{-\frac{\lambda V_2}{R}})}_{\text{Decay in Tubing}} \underbrace{\left(\frac{V_3}{1 + \frac{\lambda V_3}{R}}\right)}_{\text{Detector Chamber}} \qquad (2.1)$$

where:

DR = Decay rate (dps)

A_0 = Saturated activity (dps/ml.)

λ = Decay constant = .0976 $sec.^{-1}$

V_1 = Irradiation chamber volume (ml.)

V_2 = Volume of flow tubing from irradiation chamber to detector chamber (ml.)

V_3 = Volume of detector chamber (ml.)

R = Flow rate (ml./sec.)

If, instead of perfect mixing, slug flow occurs inside the detector chamber, the decay rate is given by:

$$DR\ slug = \underbrace{A_0(1 - e^{-\frac{\lambda V_1}{R}})}_{\text{Irradiation Chamber}} \underbrace{(e^{-\frac{\lambda V_2}{R}})}_{\text{Decay in Tubing}} \underbrace{\frac{R}{\lambda}(1 - e^{-\frac{\lambda V_3}{R}})}_{\text{Detector Chamber}} \qquad (2.2)$$

In order for equations 2.1 and 2.2 to predict meaningful results, the flow rate must be accurately known. The rotameter type flow meter was therefore checked for accuracy by measuring flow rate with a

graduated beaker and stop watch, and comparing the results to the values inscribed on the rotameter tube. The results of this check are shown ir Table 2.2, from which it may be seen that the accuracy of previous flow meter readings was poor, and probably a considerable factor in the above mentioned inconsistency in optimum flow rate determination.

Table 2.2

Calibration of Rotameter

Meter Reading	True Flow Rate	
10.0 GPH	7.8 GPH	8.22 ml/sec.
9.0	7.0	7.38
8.0	6.2	6.52
7.0	5.4	5.68
6.5	5.0	5.26
6.0	4.7	4.95
5.5	4.3	4.53
5.0	3.9	4.10
4.5	3.5	3.68
4.0	3.1	3.27
3.5	2.7	2.85
3.0	2.3	2.42

Hereafter, in this report, only corrected flow rates will be employed.

The volumes V_1 and V_2 were measured and found to be 95 ml. and 43.5 ml. respectively. The correct value for V_3 was somewhat more difficult to determine. Figure 2.4 shows a cross section view of the detector chamber. A measurement of outside dimensions indicated

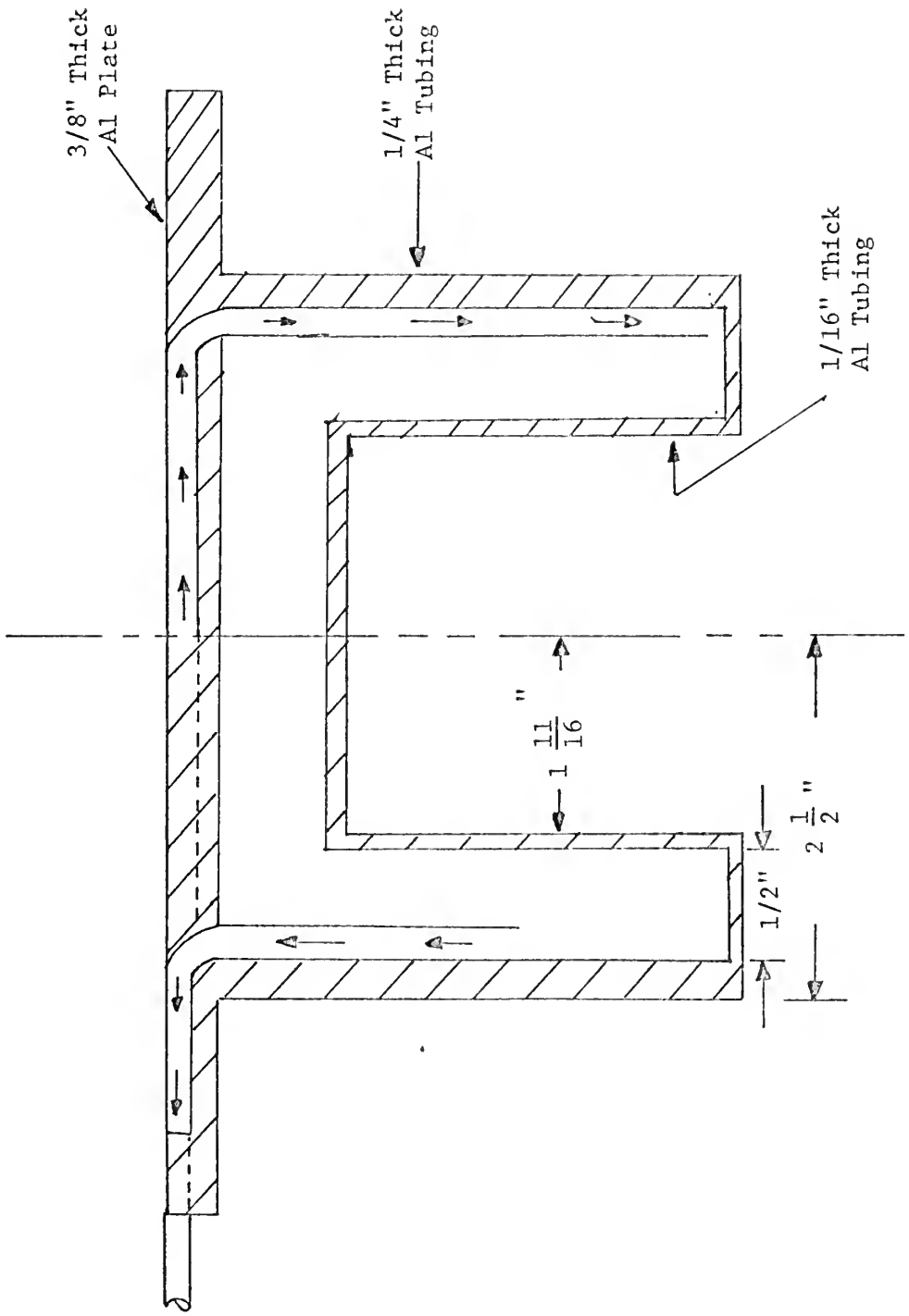

Figure 2.4

Vertical Section Through the Detector Tank

that the dimensions stated in Ref. 1 are in error. The correct dimensions are shown in Fig. 2.4. Note that the placement of the inflow and outflow tubes allows air to be trapped in the chamber, preventing it from being completely filled with water. Mestemaker used 354 ml. for V_3 of his calculations; the volume of the detector chamber as indicated by Mestemaker's diagram of the chamber in Ref. 1 is 897 ml., the volume indicated by the corrected cross section diagram in Fig. 2.4 is 462 ml., while the volume actually measured by draining out the water was 80 ml; and the volume later achieved by venting the air was 400 ml! Thus it is no wonder that the original calculation of optimum flow rate was in error.

The volume of water in the detector chamber during the previous experiments was then 80 ml. plus an additional amount due to compression of the air in the chamber by back pressure in the flow tubes. The back pressure is the result of 1.) the static head of water above the detector chamber, and 2.) the dynamic pressure head due to wall friction in tubing downstream of the chamber.

The volume of compression due to the static head was measured in the following manner: With a valve immediately upstream of the chamber in the closed position, water was bled from the drain, which is immediately downstream of the chamber. As the water above the chamber drained out, the static head was relieved, allowing the compressed air to expand and discharge the additional water out of the chamber and through the drain. Thus the volume of water collected at the drain was equal to the volume in the tube above the drain plus

the volume of static head compression. The volume collected at the drain was 28.8 ml.; the calculated volume of the tubing downstream of the drain was 10.3 ml.; and thus the volume of compression due to the static pressure head was the difference, or 18.5 ml.

The volume of compression due to dynamic pressure was measured at various flow rates by instantaneously cutting off the flow with a toggle valve upstream of the chamber and collecting the overflow at the purge tank. The volume of the overflow is equal to the volume of compression due to dynamic pressure head. The results obtained by applying these corrections are found in Table 2.3.

Using corrected values of flow rate and detector chamber volume, activity in the detector chamber is computed from equations 2.1 and 2.2 and may be found in Tables 2.4 and 2.5.

Since the detector efficiency is not known, the decay rates derived in these tables cannot be converted into count rates. However, the shape of the curves may be compared by looking at certain relative count rates and predicted activities. For example, consider the ratio of the count rate at 6.2 GPH to that at 2.3, 3.9, and 5.4 GPH respectively. It is to be expected that these ratios will be very close to the corresponding ratios of activity as predicted by equations 2,1 and 2,2. Since ratios are employed, all multiplicative constants, the detector efficiency in particular, will cancel. This comparison is shown in Table 2.6.

These results indicate that the system performance was finally adequately understood, that the difference between slug and mixed flow in the detector chamber is not significant, and that the flow rate to

Table 2.3

Data Necessary to Correct for Air Compression
In Detector Chamber

		Flow Rate	Over Flow At Purge Tank	Total Volume Correction	Resultant Detector Volume
Vol. Collected at Drain:	28.8 ml.				
Computed Vol. of Tubing Down-Stream of Drain:	10.3 ml.	6.2 GPH	15.0 ml	33.5 ml	113.5 ml
		5.4 GPH	10.0 ml	28.5 ml	108.5 ml
		3.9 GPH	7.0 ml	25.5 ml	105.5 ml
Volume Due to Static Compression:	18.5 ml.	2.3 GPH	4.0 ml	22.5 ml	102.5 ml
Volume of Detector Chamber at Atmospheric Pressure:	80 ml. (measured)				

Table 2.4

Computation of Decay Rate in Detector Chamber Assuming Perfect Mixing

From Eqn. 2.1: $\frac{DR\ mixed}{A_0} = (1 - e^{-\frac{\lambda V_1}{R}})(e^{-\frac{\lambda V_2}{R}})(\frac{V_3}{1 + \frac{\lambda V_3}{R}})$

$\lambda = .0976\ sec^{-1}$ $V_2 = 43.5$ ml

$V_1 = 95$ ml. V_3 = as per Table 2.3

R GPH	R $\frac{ml}{sec}$	V_3 ml	$\frac{\lambda V_3}{R}$	$1+\frac{\lambda V_3}{R}$	(I) $\frac{V_3}{1+\frac{\lambda V_3}{R}}$	(II) $e^{-\frac{\lambda V_2}{R}}$	$e^{-\frac{\lambda V_1}{R}}$	(III) $1-e^{-\frac{\lambda V_1}{R}}$	$\left[(I)\cdot(II)\cdot(III)\right]$ $\frac{DR}{A_0}$
6.2	6.52	113.5	1.699	2.699	42.05	.521	.242	.758	16.6
5.4	5.68	108.5	1.864	2.864	37.88	.473	.196	.804	14.4
3.9	4.10	105.5	2.51	3.51	30.06	.355	.1045	.8955	9.56
2.3	2.42	102.5	4.13	5.13	19.98	.173	.0218	.9782	3.38

Table 2.5

Computation of Decay Rate in Detector Chamber, Assuming Slug Flow

From Eqn. 2.2: $\frac{DR\ slug}{A_0/\lambda} = R(1 - e^{-\frac{\lambda V_1}{R}})(e^{-\frac{\lambda V_2}{R}})(1 - e^{-\frac{\lambda V_3}{R}})$

$\lambda = .0976\ sec^{-1}$ $V_2 = 43.5$ ml.

$V_1 = 95$ ml. V_3 = as per Table 2.3

	[I]				[II]	[III]		[IV]	$\left[\begin{matrix}(I)\cdot(II)\cdot\\(III)\cdot(IV)\end{matrix}\right]$
R GPH	$R\ \frac{ml}{sec}$	V_3 ml.	$\frac{\lambda V_3}{R}$	$e^{-\frac{\lambda V_3}{R}}$	$1-e^{-\frac{\lambda V_3}{R}}$	$e^{-\frac{\lambda V_2}{R}}$	$e^{-\frac{\lambda V_1}{R}}$	$1-e^{-\frac{\lambda V_1}{R}}$	$\frac{DR}{A_0/\lambda}$
6.2	6.52	113.5	1.699	.183	.817	.521	.242	.758	2.10
5.4	5.68	108.5	1.864	.155	.845	.473	.196	.804	1.83
3.9	4.10	105.5	2.51	.0811	.9189	.355	.1045	.8955	1.198
2.3	2.42	102.5	4.13	.0160	.9840	.173	.0218	.9782	.403

Table 2.6

Comparison of Experimental and Predicted Activity Ratios

Flow Rate Ratios	Experimental Results	Predicted Results	
		Mixed Flow	Slug Flow
6.2 : 2.3 GPH	6.77	5.2	4.91
6.2 : 3.9 GPH	1.98	1.75	1.74
6.2 : 5.4 GPH	1.214	1.15	1.15

produce a maximum count rate is well above the values considered.

2.5 Venting the Detector Chamber

The variation of detector chamber volume, V_3, with flow rate, as described in section 2.3, was considered unacceptable. It was therefore decided to vent the chamber by drilling a small hole in the top of the chamber and tapping the hole so it could be sealed with a screw and washer. In this manner V_3 was increased to a measured value of 400 ml. [The 62 ml. discrepancy between this figure and that computed from Fig. 2.4 is probably due to slight errors in construction, and volume taken up by seam welds.]

After this modification was made, count rate was once again measured with respect to flow rate. The results are found in Table 2.7. The slug and mixed flow comparisons were made and may be found in Tables 2.8, 2.9, and 2.10. Note that at the higher flow rates, the mixed flow results are very close to the experimental values.

In Fig. 2.5, DR/A_0 for the vented detector chamber is plotted against flow rate for both slug and mixed flow. Notice that maximum activity in the detector chamber occurs at a flow rate of 23 ml/sec. (21.8 GPH) for both slug and mixed flow. Since this is well beyond the capability of the present system, operation to obtain a maximum in the activity vs. flow rate curve is not feasible.

2.6 Increase in Signal to Noise Ratio

A further advantage of venting the detector chamber was an increase

Table 2.7

Counts Attributable to N-16
Activity in the Vented Detector
Chamber (Counting time = 50 sec.)

Flow Rate	Counts*
7.0 GPH	50,176
6.2	43,070
5.4	35,300
4.7	28,880
3,9	22,912
3.1	16,370
2.3	9,200

*Background Subtracted

Table 2.8

Computation of Decay Rate in Vented Detector Chamber Assuming Perfect Mixing

$$\frac{DR}{A_0} = (1 - e^{-\frac{\lambda V_1}{R}})(e^{-\frac{\lambda V_2}{R}})\left(\frac{V_3}{1 + \frac{\lambda V_3}{R}}\right)$$

$\lambda = .0976\ \text{sec}^{-1}$ $\quad V_2 = 43.5$ ml

$V_1 = 95$ ml $\quad V_3 = 400$ ml

R GPH	R $\frac{\text{ml}}{\text{sec}}$	$\frac{\lambda V_3}{R}$	$1+\frac{\lambda V_3}{R}$	(I) $\frac{V_3}{1+\frac{\lambda V_3}{R}}$	(II) $e^{-\frac{\lambda V_2}{R}}$	$e^{-\frac{\lambda V_1}{R}}$	(III) $1-e^{-\frac{\lambda V_1}{R}}$	$\left[\begin{matrix}(I)\cdot(II)\cdot \\ (III)\end{matrix}\right]$ $\frac{DR}{A_0}$
6.2	6.52	5.99	6.99	57.3	.521	.242	.758	22.7
5.4	5.68	6.87	7.87	50.8	.473	.1960	.804	19.35
3.9	4.10	9.50	10.50	38.1	.355	.1045	.8955	12.12
2.3	2.42	16.10	17.12	23.3	.1730	.0218	.9782	3.94

Table 2.9

Computation of Decay Rate in Vented Detection Chamber Assuming Slug Flow

$$\frac{DR}{A_0/\lambda} = R\left(1 - e^{-\frac{\lambda V_1}{R}}\right)\left(e^{-\frac{\lambda V_2}{R}}\right)\left(1 - e^{-\frac{\lambda V_3}{R}}\right)$$

$\lambda = .0976 \text{ sec}^{-1}$ $\quad V_2 = 43.5$ ml

$V_1 = 95$ ml $\quad V_3 = 400$ ml

	(I)		(II)	(III)		(IV)	$\left[\frac{(I)\cdot(II)\cdot}{(III)\cdot(IV)}\right]$
R GPH	$R\frac{\text{ml}}{\text{sec}}$	$e^{-\frac{\lambda V_3}{R}}$	$1-e^{-\frac{\lambda V_3}{R}}$	$e^{-\frac{\lambda V_2}{R}}$	$e^{-\frac{\lambda V_1}{R}}$	$1-e^{-\frac{\lambda V_1}{R}}$	$\frac{DR}{A_0/\lambda}$
6.2	6.52	.0025	.9975	.521	.242	.758	2.57
5.4	5.68	.0011	.9989	.473	.196	.804	2.16
3.9	4.10	.00005	.99995	.355	.1045	.8955	1.302
2.3	2.42	$\simeq 0.0$	$\simeq 1.0$	.173	.0218	.9782	.409

Table 2.10

Comparison of Experiment and Predicted Activity Ratios

For Vented Detector Chamber

Flow Rate Ratios	Experimental Results	Predicted Results	
		Mixed Flow	Slug Flow
6.2 : 2.3 GPH	4.69	5.76	6.28
6.2 : 3.9 GPH	1.88	1.870	1.974
6.2 : 5.4 GPH	1.22	1.171	1.189

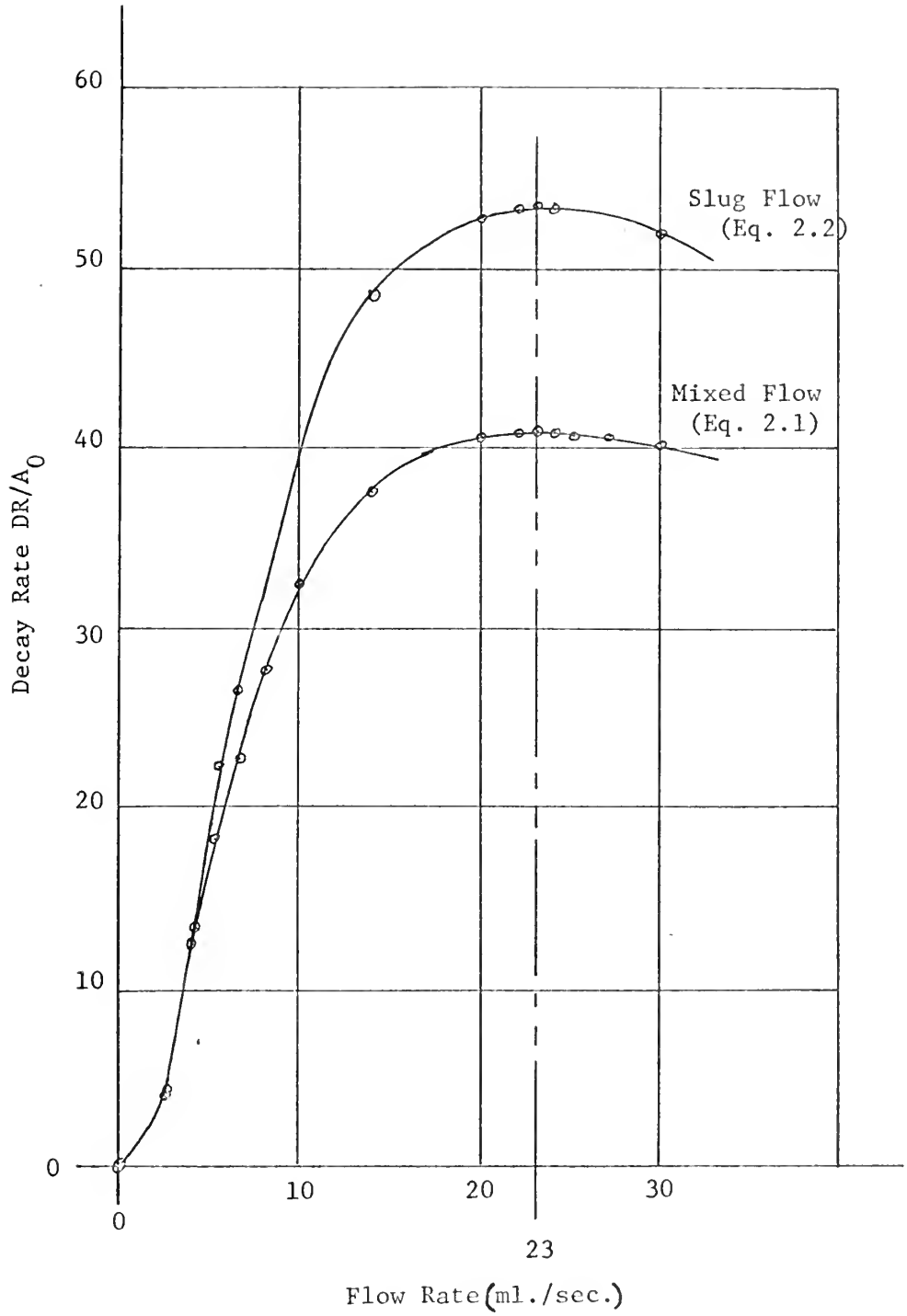

Figure 2.5

Decay Rate Vs Flow Rate
(From Eqs. 2.1 and 2.2)

in the signal to noise ratio from 2.5 in the original system to a value of 4.45 at maximum flow rate for the vented system.

2.7 Effect of the Unequal Flow Volumes of the Filters

In the original arrangement, the filter bank consisted of three one-half inch diameter aluminum tubes in parallel. Because of this arrangement, water directed through the outer filters has to travel an extra 11.5 inches further than water traveling through the center filter. This 11.5 inches represented a 3.6 ml. increase in the value of V_2 in Eqs. 2.1 and 2.2. Thus the count rate in this case was reduced by a factor of $e^{-\frac{\lambda\ 3.6}{R}}$ due to this longer flow path. The reduced activity appeared to represent N-16 removal by the material in the outer filters and therefore tended to bias the results. Another factor which could lead to a similar error is the difference in volume occupied by the various filter materials. For example, the ion exchange resin beads occupy about 1 ml. more volume than do the glass beads. This means that the flow volume through the filter itself was 1 ml. less for the outer filters, thereby reducing the extra flow volume through these filters from 3.6 to 2.6 ml. At 5.4 GPH (5.7 ml./sec) the resulting bias was $e^{-\frac{(.0976)(2.6)}{5.7}} = .9565$. Thus the value of N-16 removal calculated from the data could have been too large by as much as 4.5%, depending upon the amount of removal.

In order to reduce this error, the two side filters were brought closer to the center, as per Fig. 2.2, so that the additional flow volume for the outer filters was reduced from 3.6 ml. to 1.6 ml. When the 1 ml. difference in volume occupied by the filter materials

is included, the net difference in flow volume is reduced to 0.6 ml. At 5.4 GPH, the N-16 count rate from the outer filters is biased by the factor $e^{-\frac{(.0976)(.6)}{5.7}} = .99$. Thus the value for N-16 pickup is overestimated by less than 1%. At a flow rate of 2.7 GPH the overestimation will be less than 2%. This is considered acceptable, since it is estimated that the error introduced by imprecise control of flow rate over the course of an experimental run may be as high as 5%. [It should be noted that this latter uncertainty would not be this large if it were possible to operate at the peak of the broad maximum in the activity vs. flow rate curve, as originally intended by Mestemaker].

2.8 Effect of Aluminum System

The possibility that an aluminum oxide film inside the aluminum tubing of the N-16 facility could effect some change in the N-16 chemical distribution through selective pickup or chemical interaction, should not be overlooked. Any such effect would bias the results so that they would be peculiar to the present N-16 facility.

To investigate this possibility, two experiments were carried out:

1.) A tygon tubing in-pile-section, constructed by I.A. Forbes and described in Ref. 5, was inserted into the MITR Hohlraum and connected to the present out-of-pile section. Since all other conditions were identical, a difference in results could only be attributable to the absence of aluminum (or the presence of tygon).

N-16 removal was measured for H^+ and OH^- resins and compared to

corresponding data obtained with the aluminum in-pile section. This comparison is shown in Table 2.11 below.

Table 2.11

Comparison of Results Using Tygon

and Aluminum In-Pile Sections

Comments	Flow Rate	N-16 Removal	
		H^+ Resin	OH^- Resin
Tygon In-Pile	4.3 GPH	43%	81%
Al. In-Pile	5.4 GPH	37%	79%
Al. In-Pile (days later)	5.4 GPH	39%	76%

Note that there appears to be a slightly increased removal by the H^+ resin, but the difference is so close to the estimated 5% experimental error that it cannot be considered significant.

2.) A second experiment involved measuring N-16 removal by aluminum oxide. Al_2O_3 in the form of bubble grain alumina was inserted in one outer filter column. At 3.9 GPH the percentage of N-16 removed was measured to be 4%. Thus there may be some slight N-16 pickup by aluminum oxide, but the magnitude is again within experimental accuracy. The possibility of an aluminum oxide effect on the results should, nevertheless, be kept in mind in the construction of any future N-16 facility where greater accuracy is desired.

2.9 Summary

Various items that might possibly bias the results of experiments with the MIT N-16 facility were investigated, including: inaccuracy in flow rate measurements, variation in detector chamber volume with flow rate, unequal flow volumes through different filters, and the effect of an aluminum oxide film inside the flow tubing. The magnitude of error in each case was estimated and modifications to reduce the error were made where needed, until it was felt that no single error was greater than experimental uncertainty. Predicted activity correlated reasonably well with experimental results. Thus, it is felt that in carrying out the investigation of the built-in bias of the N-16 facility, the detailed operating characteristics of the facility were brought clearly to light and adequately understood. In the following chapter the experimental program carried out using the modified facility will be discussed.

CHAPTER III

N-16 WATER CHEMISTRY

3.1 Introduction

The formation of N-16 from O-16 in water causes the dissociation of the water molecule. The N-16 atom is thus initially in a free form, but possesses a great deal of kinetic energy as a result of the original nuclear reaction. After dissipation of this energy the N-16 atom combines immediately to form ions or neutral species. In a power reactor, gamma catalysis will accelerate this recombination and influence the resultant distribution of N-16.

Experience gained in the production of nitric acid indicates that nitrogen combines with oxygen in all its valence states from two to five. Furthermore, equilibrium between the various combinations of nitrogen and oxygen is so rapid that it is virtually impossible to use any of the oxides of nitrogen in the completely pure state without the presence of at least small amounts of the others. This equilibrium is expressed by the following equations:

$$NO_2 + NO \rightleftarrows N_2O_3 \tag{3.1}$$

$$2NO_2 \rightleftarrows N_2O_4 \tag{3.2}$$

$$N_2O_4 + H_2O \rightleftarrows HNO_3 + HNO_2 \tag{3.3}$$

$$3HNO_2 \rightleftarrows HNO_3 + 2NO + H_2O \tag{3.4}$$

$$2NO + O_2 \rightleftarrows 2NO_2 \tag{3.5}$$

If hydrogen overpressure is used to retard corrosion in the

primary cooling loop, the excess hydrogen may combine with the nitrogen to form ammonia:

$$N_2 + 3H_2 \rightarrow 2NH_3 \qquad (3.6)$$

which in turn forms ammonium hydroxide:

$$NH_3 + H_2O \rightarrow NH_4OH \qquad (3.7)$$

which ionizes partially:

$$NH_4OH \rightleftarrows NH_4^+ + OH^- . \qquad (3.8)$$

Some free oxygen is always present due to the dissociation of water caused by gamma or neutron interaction with the water molecule. This oxygen may combine with the energetic atom to form nitric acid:

$$2N_2 + 2H_2O + 5O_2 \rightarrow 4HNO_3 \qquad (3.9$$

which ionizes completely:

$$HNO_3 \rightarrow H^+ + NO_3 .$$

By virtue of the equilibrium expressed in equations 3.1 through 3.5, it is expected that some N-16 will also be in the form of NO, NO_2, N_2O_3, N_2O_4, and HNO_2.

This is confirmed somewhat by an attempt to determine the N-16 chemical distribution made by J.J. Schleiffer and J.P. Adloff who induced N-16 activity in water with 14 MeV neutrons produced by an accelerator (10). A GM tube was employed to detect the N-16 hard beta rays. Volatile forms of N-16 were separated from non-volatile forms by the use of a stripping gas, and then analyzed by the use of gas chromatography. The distribution among the non-volatile forms was

ascertained by employing various ion exchange resins and two forms of activated alumina. As a result of this work, Schleiffer and Adloff reported the chemical distribution of N-16 in pure water to be as follows: 1% N_2, 9% NO, 30% NH_4^+, 16% NH_2OH, 25% NO_3^-, and 10% NO_2^-.

3.2 Influencing the Chemical Distribution

If the various factors that control the chemical distribution were completely known, it might be possible to favorably influence the distribution in order to effect more complete removal by a particular filtering agent. As an example, consider that a particular filtering agent readily removes ammonium ions. From the discussion in section 3.1 it appears that providing a hydrogen overpressure will result in a higher percentage of N-16 in the form of ammonium ions, thus enhancing N-16 removal by this particular filter.

This effect was indeed observed by R. L. Mittl and M. H. Theys, who studied N-16 water chemistry in EBWR (17). Using anion and cation ion exchange resins, they reported that in pure water N-16 combines mainly in the anion form, the ratio of anion species to cation species in the water being 7 to 1. (Note that this is in contrast with the distribution reported by Schleiffer and Adloff.) Nitrogen, oxygen, and argon gas had no apparent effect on the ion form of N-16. The addition of hydrogen gas, hydrazine, or ammonia decreased the anion to cation ratio in the water. At 20 MW (th), 600 psig and 489°F, the addition of 40 cm^3 of H_2 per liter of feedwater led to nearly equal proportions of anions and cations in water.

In apparent conflict with these results are the results of the previous series of experiments with the MIT N-16 facility by the author, summarized in Chapter II of this report. Of interest is the apparent alteration of the ratio of anions to cations after nitrogen and helium gas purges. N-16 removal was first measured in air saturated water for H^+ and OH^- ion exchange resins (the implication being that the H^+ resin will selectively remove cations and the OH^- resin will remove anions). The system was then purged with nitrogen gas to strip out all dissolved gases but nitrogen, and N-16 removal again measured. This procedure was then repeated with helium gas. Table 3.1 shows the results of this experiment.

Table 3.1

Effect of Gas Purges in Previous Experiments with N-16 Loop

Purge Gas	N-16 Removal	
	H^+ Resin	OH^- Resin
Air	38%	86%
Nitrogen	38%	60%
Helium	48%	74%

The implication of Table 3.1 is that the presence or absence of dissolved nitrogen and oxygen significantly affects the amount of N-16 activity in the anion form, and to a lesser extent, in the cation form.

On the basis of the apparently positive results indicated in Table 3.1, it was decided to continue with this line of investigation using the modified N-16 facility.

3.3 Further Work Using Various Purge Gases

Having eliminated various sources of error from the N-16 loop, and in view of the contradictions in results noted above, it was considered desirable to repeat the previous experiments with nitrogen and helium purge gases in order to substantiate the results of Table 3.1. The procedure followed was:

The degree of N-16 removal by the H^+ and OH^- resins was first measured with air as the cover gas. The system was then purged with nitrogen for 15 minutes at a gas flow rate of about 2 ft^3/hr with the water flowing at the maximum rate. The exit tube of the purge tank was then sealed with tape and N-16 removal measured. The procedure was then repeated, but with a helium purge. The results are shown in Table 3.2.

In order to ensure that the purges were of long enough duration, it was calculated that about 15,000 ml. of purge gas (STP) was used in each purge. The maximum amount of gas that could be contained in the system was calculated to be (including 200 ml. for the void space above the water in the purge tank) 243 ml for H_2, 224 ml for He, 247 ml for N_2, and 298 ml for O_2. Thus in each purge more than 50 system gas volumes were circulated, and it thus appears that the purges were of sufficient duration to both strip the system of all other gases and saturate the system with the gas itself.

In Section 3.1 it was suggested that an excess of hydrogen gas could result in enhanced formation of ammonium ions, and, that similarly, an oxygen excess could result in the enhanced formation of nitrate ions. It therefore seemed a logical next step to test the

PURGE GAS	FLOW RATE	N-16 REMOVAL	
		H^+ RESIN	OH^- RESIN
None (Air Cover	5.4 GPH	39%	76%
Nitrogen	5.4 GPH	45%	71%
Helium	5.4 GPH	47%	71%
None (Air Cover)	3.1 GPH	46%	86%
Hydrogen	3.1 GPH	45%	80%
Oxygen	3.1 GPH	41%	83%

Table 3.2

N-16 Removal Following Various Gas Purges

effect of hydrogen and oxygen purges.

Due to certain MITR regulations prohibiting the use of explosives or fire hazards in the reactor area, a variation of the purge procedure was followed for these two gases. With the in-pile section in the Hohlraum, the system was purged with helium to strip the water of all possibly reactive gases. Next the out-of-pile section was separated from the in-pile section and removed from the reactor area, where a hydrogen purge was made. The cart was then wheeled back into the reactor and connected with the in-pile section, and N-16 removal measured. The procedure was then repeated, but with an oxygen purge.

Between purges the exit gas tube of the purge tank was sealed with tape to prevent contamination by the atmosphere. Note that in this procedure the 95 ml. of water in the irradiation chamber was not exposed to the hydrogen or oxygen purge, but instead contained dissolved helium. Helium, however, is chemically unreactive and should not affect the results of the purges, with the possible exception of its dilution effect on the dissolved purge gas. Since the volume of the total system is about 2000 ml., however, the dilution by the gas dissolved in 95 ml of water is not appreciable.

The results of these purges may be found in Table 3.2. Note that again no appreciable change in the N-16 distribution is evidenced.

3.4 Discussion of Results

Several other experimenters, in the process of studying N-16 water chemistry, have looked at the effect of various gas purges.

Although there is some disagreement about the proportion of anions and cations in pure water (Schleiffer and Adloff (10) reported near equal proportions, while Mittl and Theys (17) reported an anion to cation ratio of about 7 to 1.), it has been found by both groups that N_2 and O_2 purge gases have no apparent effect on the N-16 chemistry, while H_2 gas has had a noticeable effect. Schleiffer and Adloff reported that the use of a hydrogen purge nearly doubled the volatile fraction of N-16 and Mittl and Theys reported that after a hydrogen purge, nearly equal proportions of anions and cations existed in the water. Additionally, G.K. Whitham and R.R. Smith in experiments with BORAX IV found that while N_2, O_2 and He purges had no effect, an H_2 purge more than doubled the N-16 activity in the primary loop steam (18). This is a reasonable consequence of increasing the volatile fraction of N-16.

Although there is no ready explanation for the difference between the results of the previous experiments with the N-16 loop (Table 3.1) and the most recent experiments (Table 3.2), it is felt that the most recent experiments were conducted under more precisely controlled conditions, and therefore have yielded the more credible results. Nevertheless, the influence of hydrogen on the N-16 chemical distribution has not been evidenced in the work with the MIT N-16 loop.

Further discussion of this discrepancy, as well as recommendations for future water-chemistry studies with the MIT N-16 facility may be found in Chapter V.

CHAPTER IV

TESTING OF INORGANIC FILTER MEDIA

4.1 Introduction

Up to this point, N-16 removal capabilities have been demonstrated only for organic-base ion exchange resins. These materials were used in the experiments described in previous chapters to develop information concerning the chemical form of N-16 and the effect of the chemical environment upon it. These materials are not suitable for high temperature use. Therefore one major objective of the present work has been to test candidate materials which can function under more realistic operating conditions. Desirable criteria which should be met include:

1.) The material chosen must be able to withstand the high temperatures ($\simeq$ 600°F) encountered in a PWR primary coolant loop.

2.) It must be essentially insoluble in high temperature water in order not to undergo transport processes which could lead to the fouling of heat transfer surfaces, and to the contamination of plant surfaces by radionuclides produced by neutron irradiation of the constituents of the medium.

3.) It must be stable in the presence of high gamma and neutron radiation fields, particularly if it is to be considered for use in an in-pile filter.

These requirements appear to preclude the use of organic materials, which in general violate requirements 1 and 3. This leaves the inorganics as the broad category within which the search has centered.

4.2 Previous Work with Inorganic Filter Materials

Erroneously termed "ion exchangers", most of the inorganic materials to be considered pick up water-borne ions by a complicated process of adsorption whereby a valence electron, in the case of anion pickup, or an electron "hole", in the case of cation pickup, is exchanged for the removed ion. One exception is aluminosilicate ($Na_2O \cdot A\ell(OH)_3 \cdot 6Si(OH)_4 \cdot xH_2O$) which exchanges a sodium ion (11). This material has been used by the Oak Ridge National Laboratory to remove cesium from fission produce wastes. Its order of selectivity is: $Cs^+ > Rb^+ > K^+ > Na^+ > Li^+$. Although it is insoluble in neutral salt solutions, the release of sodium ions into solution by exchange is undesirable, since sodium is readily activated in a neutron flux.

Magnetite (Fe_3O_4), on the other hand, has been found to remove Fe^{59}, Co^{58}, and Co^{60} by adsorption, again at the Oak Ridge National Laboratory (14). Considered for reactor plant use as a water purifier in a small by-pass loop in parallel with the primary loop, it has the advantage of already being present as the product of corrosion in water-steel systems. Experiments at the ORNL showed that it removed most of the Fe^{59} in solution, about one-third of the Co^{58} and Co^{60}, and a small amount of Mn^{54}.

A group of inorganics that might be referred to as "hydrous metal oxides and salts" has been shown to have remarkably diversified adsorption properties. Hydrous manganese oxide ($MnO \cdot H_2O$) shows a well marked affinity series: $Cs^+ > NH_4^+ > K^+ > Na^+ > Li^+$ (12). Hydrous SnO_2, ThO_2, TiO_2, and ZrO_2 possess both anion and cation

adsorption properties. ThO_2 and ZrO_2 adsorb cations which readily form bonds with oxygen under acid conditions, but primarily act as anion adsorbers.

Hydrous lead sulfate has shown a remarkable adsorption capacity for both anions (8.5 meq./gram at pH 1.0) and cations (7.5 meq./gram at pH 12.5). Hydrous zirconium phosphate shows a capacity of 5 to 6 meq./gram in alkaline solutions. Its order of selectivity is $Cs^+ > Rb^+ > K^+$, $NH_4^+ > Na^+ > Li^+$. At a pH of 7, however, it shows a steady loss of phosphate by hydrolysis of zirconium, an undesirable property.

Previous work has shown that all of the metal oxides and salts are highly form sensitive, with maximum adsorption capacity in the fully hydrated form. Most of the materials mentioned are completely inactive in the anhydrous form. Preparation by precipitation from a salt solution by the addition of the proper acid or base results in a fully hydrated form. The degree of hydration, and hence the adsorptopn capacity and adsorption rate, depends on the drying temperature and time. In the case of titanium dioxide, the removal of water is reversible up to a point beyond which further drying results in the collapse of the matrix to a configuration with a higher density. This is accompanied by a marked decrease in capacity to adsorb uranium ions, but little change in the capacity for ions such as sodium (13).

Of the materials discussed above, three were given further detailed consideration by the author: magnetite, titanium dioxide, and zirconium dioxide.

4.3 Magnetite

Magnetite is the product of high temperature oxidation of iron, and as such is found to some small degree on the surface of stainless steel fuel element cladding and primary loop piping in a PWR. The use of magnetite in a filter thus has the advantage of introducing no new material into the reactor system. It is inexpensive, easily prepared, and thus is a logical choice for testing in the N-16 facility.

Granular magnetite was prepared by sintering fine Fe_3O_4 powder, obtained from the MIT Chemical Supply Room, at 1400°C for one hour. This resulted in a very porous mass about four times denser than the original powder. It was crushed and sieved to a particle size of 20 mesh or larger for use in the filter columns.

A good flow rate through the filter was easily achieved with a pressure drop of only 3 psi at 5.4 GPH. N-16 removal, however, was quite small with a maximum of 8% removed.

4.4 Previous Work with Titanium Dioxide.

Hydrous titanium dioxide is presently being used in England in an attempt to remove uranium from sea water (13). It was found to be primarily a cation adsorber at high pH and an anion adsorber at low pH as shown in Figure 4.1.

This behavior is more or less characteristic of all the hydrous metal oxides and salts. Adsorption rate and capacity were found to be quite form sensitive for uranium, but less so for smaller ions like sodium (and presumably ammonium). The probable explanation is that

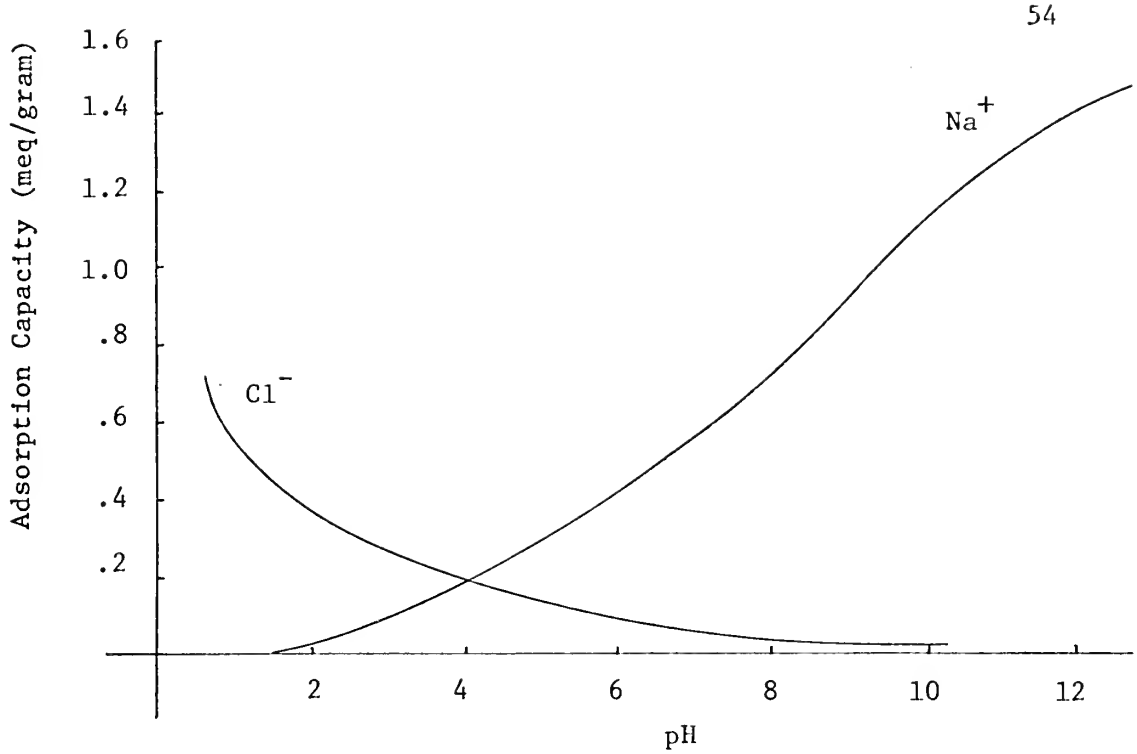

Figure 4.1

Capacity of Hydrous Titanium Dioxide
(Taken from Ref. 12)

the size of the spaces in the crystal matrix controls the ability of large ions, such as $UO_2(CO_3)_3^{-4}$ and UO_2^{+2}, to diffuse into the crystal granule. When significant water of hydration has been removed by drying, the matrix collapses to a denser form that apparently allows only the smaller ions to diffuse through it.

4.5 Preparation for Filter Use

Freshly precipitated wet floc has a high adsorption capacity and a high rate of adsorption for uranium. First attempts by the British at filter material preparation involved washing the wet floc onto glass wool fibers and then packing them into glass tubes. The low resultant density required the use of large filter sizes, and

furthermore, the floc was easily washed off the glass fibers.

Preparation of solid granules was then undertaken and the following process eventually settled upon as a standard procedure by the British workers:

1.) precipitation of hydrous titanium dioxide from a sulfate or chloride solution by the addition of alkali;

2.) washing the precipitate;

3.) drying the precipitate to a cake;

4.) crushing and sieving to a desirable particle size.

The product was obtained in the form of glassy irregular shaped granules with typical composition by weight: TiO_2 - 60%, H_2O - 35%, Na - 5%.

4.6 Preparation for Use with the N-16 Facility

An attempt at preparation of titanium dioxide for use in the N-16 facility was made as follows:

The information from Ref. 13 suggests that TiO_2 can be prepared by precipitation from sulfate or chloride solutions by the addition of alkali. Titanium sulfate and titanium trichloride (the only chloride readily available) were threfore procured. Titanium sulfate, however, was found to be essentially insoluble in pure water.

Titanium trichloride was reacted with ammonium hydroxide and a dark purple-black precipitate resulted. Titanium dioxide floc is chalky-white in color, not dark. It is therefore hypothesized that titanium sesquioxide was the dark precipitate, produced in the following

reaction:

$$2TiCl_3 + 6NH_4OH \rightarrow Ti_2O_3 + 6NH_4Cl + 3H_2O \ .$$

Due to the failure to obtain the desired precipitate, further study of titanium dioxide was abandoned in favor of zirconium dioxide, which is reported to have similar adsorption properties. This similarity is to be expected since Ti and Zr occur in the same group in the periodic table. In one regard, zirconium is the more attractive of the two since large quantities are already present in the zircaloy cladding of many PWR's. Hence ZrO_2 is already present in the system and thus of proven compatibility.

4.7 Previous Work with Zirconium Dioxide

Hydrous zirconium dioxide has been tested as an adsorber of corrosion products in the primary loop of a PWR by Westinghouse at temperatures up to 590°F (15). It was found that its adsorption capacity was high and was very insensitive to temperature. At low pH it acts as an anion adsorber and at high pH as a cation adsorber. It was also found that the adsorption properties of high-temperature-fired ZrO_2 could be restored by rehydrating it in hot aqueous solutions.

4.8 Testing ZrO_2 in the N-16 Facility

Hydrous zirconium dioxide was prepared by the author at MIT by precipitation of an aqueous zirconium nitrate solution with ammonium hydroxide:

$$Zr(NO_3)_4 \cdot 5H_2O + 4NH_4OH \rightarrow 4NH_4NO_3 + ZrO_2 + 7H_2O.$$

A chalky-white gelatinous floc resulted which, when reacted in stochiometric proportions, clogged the filter paper to the extent that the floc could not be washed. By a process of trial and error it was found that if about double the stochiometric proportion of ammonium hydroxide was used, the resulting floc was coarser and did not clog the filter paper. After washing, various methods of drying were employed:

In the first method the precipitate was placed about 12 inches under a 250 watt heat lamp for 18 1/2 hours. The result was a yellow substance, soft enough to crush between one's fingers, and which immediately broke into very fine particles when immersed in pure water.

In the second method the precipitate was dried for 18 1/2 hours in an oven at 150°C, resulting in a fairly soft crystalline substance, lighter in color than the first sample, which, upon immersion in water, appeared to effervesce and broke into very fine yellow particles. The particle size after immersion in water was, in both instances, about as small as typical table salt or sugar granules, and tended to clog the filters so that reasonable flow rates could not be obtained.

The rationalization for this behavior is that in both samples water of hydration had been reversible removed. Upon contact with water, the removed water was immediately restored, resulting in an expansion of the lattice and the subsequent crumbling of the structure. It was concluded that, in order to avoid destruction of the crystal upon contact with water, two alternatives existed: either drive off less water of hydration so that a substantial density change does not occur, or drive off more water of hydration in an attempt to form the stronger

crystal matrix that is characteristic of the high-temperature-fired ZrO_2.

The former was easily achieved by removing the ZrO_2 from the heat lamp at the first sign of a yellow tint. This required about 4 to 8 hours of exposure, depending upon the batch size. The product was rather soft but still crystalline in form as indicated by readily identifiable cleavage planes. As predicted, there was no apparent reaction upon contact with water. It was, however, too soft for use in the filter tubes, as evidenced by filter clogging when flow rates greater than 1 GPH were attempted.

The latter alternative proved very successful. After 20 hours in an oven at 300°C, a fairly hard attrition-resistant white crystalline form resulted. No reaction with water was evidenced and the crystals remained white in color under all circumstances. There was, nevertheless, some rehydration of the structure as indicated by heat given off when the material was held in a moistened hand several days after its preparation. The sample was crushed to a desirable particle size and reasonable flow rates were readily obtained. At 5.4 GPH the measured ΔP across the sample was only 5 PSI.

The sample was tested in the N-16 facility and found to remove 35% of the N-16 activity at a flow rate of 3.1 GPH, and 30% at 5.4 GPH. In an attempt to duplicate these highly favorable results, another sample was prepared in the same manner as described above and tested with the following results: 44% removal at 3.1 GPH and 38% removal at 6.2 GPH. The difference in removal percentages between the

two samples could easily be explained by a difference in average particle size, resulting in a difference in total surface area in the filter tube.

4.9 Test of pH Effect

Figure 4.1 shows the effect of pH on the adsorption capacity of TiO_2. Notice that the total capacity is lowest at a pH of about 7. Since ZrO_2 is physically and chemically very similar to TiO_2, one could expect the effect of pH to be similar for ZrO_2. This is verified to some extent by Ref. 15. It was therefore decided that N-16 pickup by ZrO_2 should be tested at both high and low pH.

The sample was first tested at a pH of 7. Next a .01N solution of LiOH was created by adding LiOH to the purge tank. pH was checked by use of pH paper and found to be about 12. N-16 removal was measured: the results are recorded in Table 4.1. The system was flushed continuously until the measured pH was once again 7 and N-16 removal measured and recorded. Finally, a .1N solution of boric acid was created and pH measured to be about 5. N-16 removal was measured and recorded.

The severe deterioration of the sample as indicated by Table 4.1 is probably the result of an early saturation of the ZrO_2 by Li^+ ions. The pH tests must therefore be considered inconclusive.

4.10 Summary

In summary, various inorganic materials, notably the hydrous metal oxides and salts, have been shown effective in removing water-

Table 4.1

Effect of pH on N-16 Adsorption by ZrO_2

Water Condition	Flow Rate	N-16 Removal
Pure water (pH 7)	5.4 GPH	37%
.01N Sol LiOH (pH 12)	5.4 GPH	2%
Pure water (pH 7) (system flushed out)	5.4 GPH	6%
.1N Sol H_3BO_3 (pH 5)	5.4 GPH	9%

borne ions by adsorption. Magnetite, titanium dioxide, and zirconium dioxide were considered good candidates for testing in the N-16 facility, although due to difficulties encountered in the preparation of TiO_2, only magnetite and ZrO_2 were actually tested. In the case of ZrO_2 the tests were highly favorable, with as much as 44% of the N-16 activity being removed in a single pass through the filter. The implications of these results will be discussed in the next chapter.

CHAPTER V

DISCUSSION OF RESULTS, CONCLUSIONS, AND RECOMMENDATIONS

5.1 Introduction

As stated in Chapter I, the objectives of this thesis were:

1.) To determine the specific characteristics of the MITR N-16 facility in order to account for any built-in bias in the data obtained.

2.) To confirm previous evidence of N-16 removal, and more accurately define the effect of cover gas on the N-16 system.

3.) To seek and test materials, such as inorganic filtering agents, that will remove significant amounts of N-16 activity and still be chemically stable at PWR operating temperatures.

The work leading to the accomplishment of each of these objectives has been presented in Chapters II through IV. This chapter is intended merely to highlight these previous chapters by providing a discussion of some of the more interesting results, conclusions, and contradictions, as well as to provide recommendations for future work in this area.

5.2 Sensitivity to Flow Rate

The highest flow rate readily achievable with the present N-16 facility is about 6.2 GPH (6.5 $\frac{ml}{sec}$). Figure 2.5, however, indicates that at this flow rate we are operating along the steepest portion of the activity vs. flow rate curve. Hence small variations in flow rate over the course of an experimental run result in rather large variations

in count rate. This is probably the explanation for variations in measured N-16 activity of as much as 5-8% from one run to another. This rather large experimental error could be significantly reduced if the system could be operated in the region of the broad maximum in the activity vs. flow rate curve. Note that for the case of mixed flow, the curve is nearly flat between R = 20 ml/sec (19 GPH) and R = 30 ml/sec (28.5 GPH). Small variations in flow rate in this region would have almost no effect on the N-16 count rate, thus reducing experimental uncertainty to the level of statistical uncertainty (about 1% or less in most of the recent N-16 loop experiments).

This range of optimum flow rates is well beyond the capability of the present system. It has been calculated, however, that if the volume of the detector chamber were reduced to 80 ml, the optimum flow rate would be reduced to about 12 GPH (12.7 ml/sec), at the expense of about a 40% reduction in the signal to noise ratio. By using a more powerful pump, and decreasing the length of the filter tubes while increasing their diameter, a flow rate of 12 GPH might be achievable. The enhanced activity level at the detector chamber associated with the greater flow rate would more than counter the effect of the reduced signal to noise ratio, and the experimental error thereby be reduced to about 1%.

5.3 Effect of Aluminum Oxide

In Chapter II it was suggested that $A\ell_2O_3$ in the N-16 system

might possibly influence the data obtained. Although tests of N-16 pickup by alumina in the N-16 facility proved negative, it is evident from the work of Schleiffer and Adloff (10) that different chemically active forms of alumina exist which definitely effect selective N-16 removal. It is thus necessary to further explore the possibility of an aluminum oxide effect on the data obtained with the N-16 facility.

5.4 Results of Water Chemistry Studies

The results of the water chemistry studies carried out with the N-16 facility in conjunction with this thesis were, for the most part, in accord with the results reported in the literature. It was verified that oxygen, nitrogen, and helium gases had virtually no effect on N-16 distribution. The results of the hydrogen gas purge, however, are in conflict with the reported results of at least three other independent studies (10), (17), (18). It has been noted that in most instances the other experimenters used other than H^+ and OH^- ion exchange resins, the sodium and chloride forms in particular. It may be that in the H^+ and OH^- form the resins are not sensitive enough. In any event, it seems that a repeat of the hydrogen gas experiment with other ion exchange resins is warranted, particularly in view of the fact that hydrogen gas is commonly used as an additive to PWR primary coolant loops.

Another possible explanation is that the experiments reported in the literature, particularly the reactor experiments, were carried out under conditions of very high radiation density, resulting in high

free radical concentrations in the water. The N-16 loop, on the other hand, operates at very low power, and would therefore have a much lower free radical concentration. This possible cause for the discrepancy should be investigated in future work.

5.5 The Inorganic Filter Materials

It was in the investigation of various suitable filtering materials that the most significant success of this endeavor was realized. The discovery that a hydrous form of zirconium dioxide would remove up to 44% of the N-16 activity in solution is a significant step in the search for a means of removing N-16 activity from reactor cooling water. It is also in this area that the greatest amount of "follow up" is called for.

The possibility of using a hydrous (active) form of magnetite must not be overlooked (the form tested in this study was a sintered, anhydrous form); hydrous titanium dioxide must be synthesized and compared with zirconium dioxide; the process for preparation of zirconium dioxide must be optimized; the effect of pH on N-16 removal must be investigated; and, finally, the most promising form of inorganic filtering material must be tested under operating conditions more closely simulating those in the primary coolant loop of a PWR, particularly in regard to temperature and radiation density.

5.6 Specific Recommendations for Future Work

The following specific recommendations for future work with the MIT N-16 facility are submitted:

1. An improvement of the N-16 loop in order to operate at optimum flow rate is warranted. The following changes toward this end should be considered: reducing the detector volume, altering the filter-tube configuration to reduce pressure drop, switching to a more powerful pump, and employing larger diameter flow tubes to reduce pressure drops.

2. Additional experiments in influencing the N-16 chemical distribution are recommended. The effect of hydrogen, hydrazine, and ammonia on N-16 water chemistry should be studied using various ion exchangers and adsorbers in an attempt to verify the results reported in the literature.

3. An attempt should be made to obtain magnetite, alumina, and other inorganic oxides in hydrous form and test their effect on N-16 removal.

4. Hydrous titanium dioxide must be tested. It is suggested that titanium tetrachloride (which is the starting form employed by the British workers) be procured and reacted with ammonium hydroxide. Additionally, titanium sulfate should be tested for solubility in mild acids and bases, and in partial alcohol solutions so that TiO_2 might be precipitated in hydrous form.

5. Direct oxidation of titanium and zirconium metal should be attempted by using hydrogen peroxide, oxidizing acids, and by heating in pure oxygen. In this manner non-friable particles of the proper diameter, which would be very compatable for filter column use, could easily be produced.

6. Finally, it is suggested that further investigations into the preparation of ZrO_2 (and TiO_2) in crystalline forms be carried out. Attention should be given to the possibility of a rehydration process that would increase the capacity for N-16 adsorption.

5.7 Conclusion

In conclusion, the results obtained during the course of the present work have been sufficiently encouraging to suggest that the ultimate objective of developing a practical N-16 removal system for pressurized water reactors may well be possible, and that indeed a higher priority should be given to continuation of this work.

APPENDIX A

ALTERNATE DETECTORS

A.1 Cerenkov Detector

As is shown by Fig. 1.1, the decay energy of N-16 is 10.4 MeV. Direct beta decay to the ground state of O-16 occurs with a probability of 26%. In these decays, a spectrum of high energy beta rays is given off with E-max. equal to 10.4 MeV. Thus, whenever N-16 activity is present, there is also present a relatively high flux of high-energy beta particles. Since the N-16 considered in this thesis is contained in water, production of visible Cerenkov radiation by these beta particles will occur. Background competition should be minimal since there is essentially no high energy beta background, and the probability of a high energy background gamma having an interaction in the small detector volume of water is small. Even when a gamma interaction occurs, the amount of Cerenkov radiation subsequently produced will usually be small since the kinetic energy of the scattered electron will usually be considerably less than that of the incident gamma.

Figure A.1 shows the simple Cerenkov detector used to test this idea. It consists of a small water hold-up tank with a plexiglass window mounted with silicon grease to a photo tube. This assembly is inserted in a tin can and sealed light-tight with gray tape.

Fig. 4.1 Cerenkov detector apparat

A.2 Results of Cerenkov Test

The Cerenkov detector was connected to the N-16 facility immediately downstream of the filter bank and the entire system operated according to standard procedures discussed in Appendix C. The base line of the linear amplifier was set very low in order to accept the low pulse heights anticipated from Cerenkov radiation. Unfortunately, at this low base line setting there was a great deal of interference due to brush-arcing in the electric pump motor. No counts above this interference level could be ascertained and the experiment therefore proved to be inconclusive (7).

Note that this attempt at a Cerenkov detection system was only a first iteration, and a crude one at that. It is felt that further work is warranted in this area and it is recommended that particular attention be paid to designing a photo tube and counting electronics that are especially sensitive to Cerenkov radition. Since the low energy of Cerenkov radiation precludes any high level discrimination, it is recommended that an induction motor be used to drive the water pump, thereby eliminating the noise due to brush arcing. [It should be noted that Cerenkov radiation from N-16 beta's has successfully been monitored by other experimenters (8).]

A.3 N-17 Neutron Detection

Note from Table 1.1 that a small amount of N-17 is produced in the reactor cooling water. Although the N-17 activity is only about one five-thousandth that of N-16, N-17 beta decays to O-17, which gives off a neutron 95% of the time and returns to stable O-16. The

emitted neutrons should be easily detected in a properly shielded chamber. Although shielding is required because of the relatively high neutron background in the MITR, this can be accomplished by the use of paraffin, which is realtively light in weight, and a thin cadmium sheathing. The paraffin also serves to moderate the N-16 neutrons which may then be detected with a BF_3 tube.

This type of N-17 neutron detection has been effectively employed at the IRR-1 swimming pool reactor where it was used to monitor reactor power (9). The detector was attached to the coolant pipe between the pool outlet and the primary circulating pump. Pulse height discrimination was employed and the detector was found to be insensitive to the gamma background.

Figure A.2 shows the N-17 detector equipment constructed for use in this experiment. It consists of an annular water detector tank surrounded with paraffin in a five gallon can sheathed in cadmium. A BF_3 tube was inserted in the center of this apparatus to detect the slow neutron flux in the paraffin.

The equipment was set up according to the schematic of Fig. A.3. A high background count was observed. This was attributed to a high energy neutron flux leaking from the MITR which penetrated the cadmium sheath. The entire detector bucket was therefore surrounded with paraffin bricks in order to slow down the externally incident neutrons to facilitate capture by the cadmium. The background was thereby reduced to a relatively low 900 counts per minute (compared to 14,000 cpm with the gamma detector).

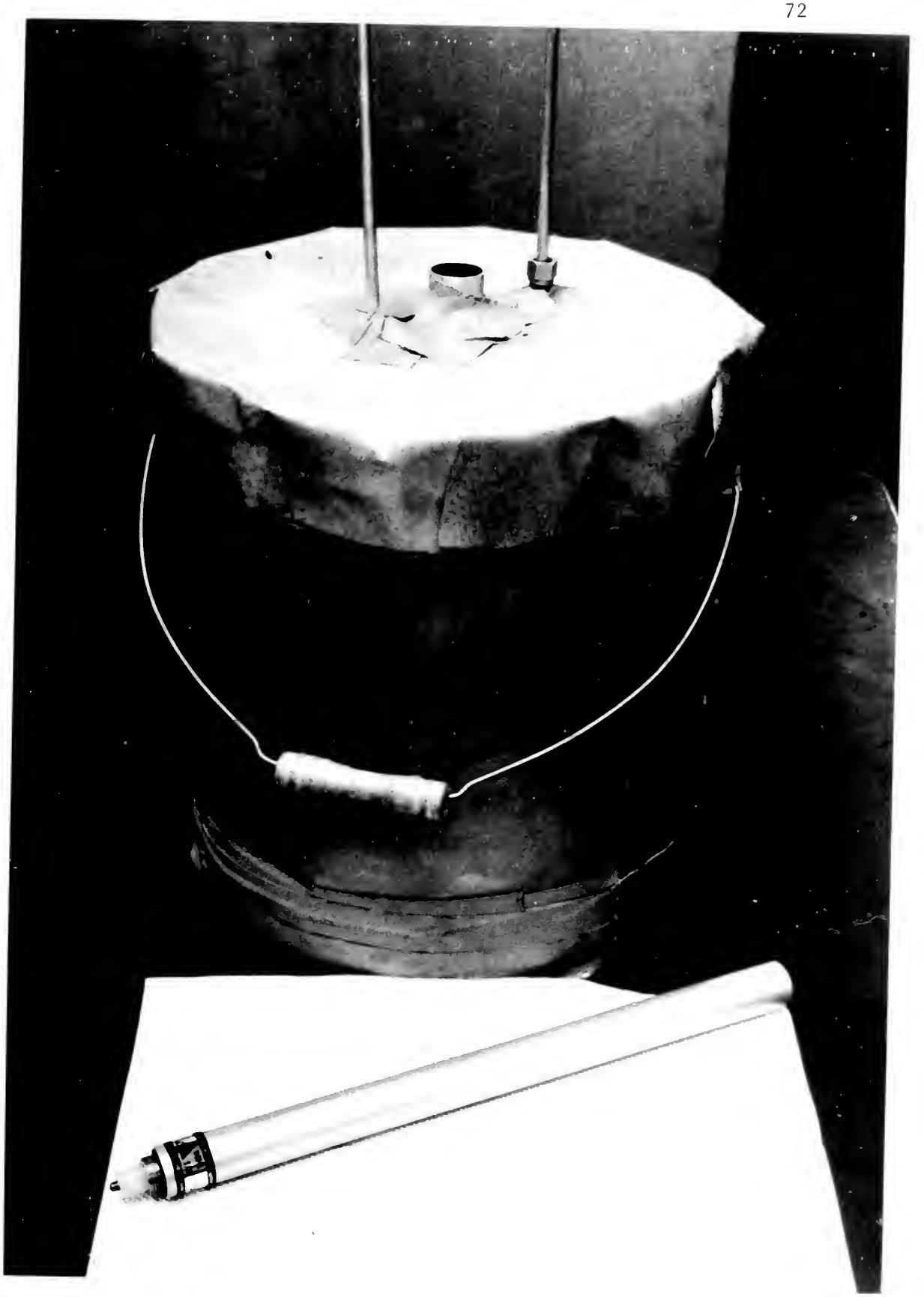

Fig. A.2 N-17 Detector Equipment

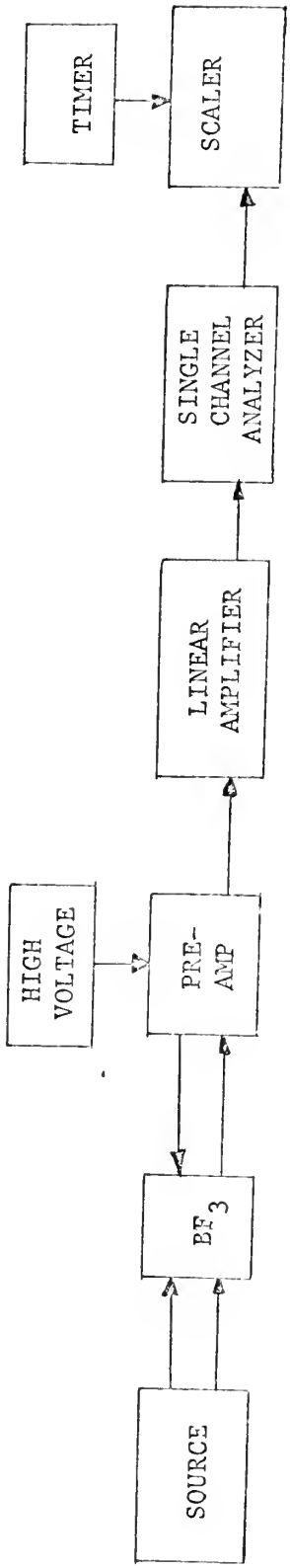

Figure A.3

Schematic of Equipment

For N-17 Detector

At this point it became clear that the subject N-17 detector would not be adequate. Table 1.1 indicates that N-17 activity in reactor water is about $\frac{1}{5000}$ that of N-16. The N-16 count rate achieved previously with the gamma detector was about 25,000 cpm. Assuming roughly equal overall detection efficiencies for neutrons and gamma rays, one would not expect much more than a 5 cpm signal from the N-17 neutrons. This is completely indistinguishable above the background of 900 cpm. This result was indeed obtained when the apparatus was tested in service - no signal above background could be detected (7).

This means of detection, while undoubtedly feasible for a higher power system, appears to be impracticable, due to low count rates, in a small scale, low power mockup such as the present N-16 facility. For that reason it is recommended that any future detector development work be concentrated on the Cerenkov type systems.

A.4 Feasibility of Beta Detection Systems

Since N-16 undergoes beta decay with E-max equal to 10 MeV and $\bar{E}$ equal to about 3.3 MeV, it should be possible to use various beta detection schemes to monitor N-16 activity.

For example, as suggested in Ref. 10, a GM detector can be used. The range of 2 MeV beta particles in aluminum is about 6 mm (1500 mg/cm^2). Thus a thin walled annular water chamber should transmit a significant beta signal. These betas should also be capable of penetrating the GM tube wall.

The thickness of the water annulus should be about equal to the maximum range of 10 MeV beta particles in water, about 5 cm (5000 mg/cm^2).

The above detection system should be more compact, easier to shield, and less sensitive to gamma ray background that the present NaI system.

Another possibility, that should have an even lower background, is a surface barrier silicon detector covered by a thin window. Since the N-16 disintegration rate at the detector chamber is approximately 500 cps/cc, the small size of these detectors may not prove detrimental to the achievement of reasonable count rates. This detector could be used with a detector chamber as small as 3 cm. radius and 3 cm. thickness.

Another detector worthy of consideration is a plastic scintillator, drilled out to provide a water passage.

APPENDIX B

CALCULATION OF ACTIVITY IN THE DETECTOR CHAMBER

B.1 Definition of Terms

P = Production rate per ml. $(\frac{1}{\text{sec ml}})$.

DR = Decay rate per ml. $(\frac{1}{\text{sec ml}})$.

A = Activity $(\frac{\text{dps}}{\text{ml}})$.

A_0 = Saturated activity $(\frac{\text{dps}}{\text{ml}})$.

Σ = Macroscopic cross section $(\frac{\text{cm}^2}{\text{ml}})$.

N = N-16 concentration $(\frac{\text{N-16 atoms}}{\text{ml}})$.

ϕ = Flux in irradiation chamber $(\frac{\text{fast neutrons}}{\text{cm}^2 \quad \text{sec}})$.

R = Flow rate $(\frac{\text{ml}}{\text{sec}})$.

λ = N-16 decay constant (sec^{-1}).

V_1 = Irradiation volume (ml.)

V_2 = Flow volume from irradiation chamber to detector chamber (ml.)

V_3 = Detector chamber volume (ml.)

Note that where applicable, values are taken on a "per ml." basis.

B.2 Activity Produced in the Irradiation Chamber

$$P = \phi\Sigma = \frac{\text{N-16 atoms produced}}{\text{sec ml}} \tag{B.1}$$

$$DR = N\lambda = \frac{\text{N-16 atoms decaying}}{\text{sec ml}} \tag{B.2}$$

$$\frac{dN}{dt} = \text{Production rate - decay rate}$$

or:
$$\frac{dN}{dt} = \phi\Sigma - N\lambda \tag{B.3}$$

Rearranging:

$$\frac{dN}{\phi\Sigma - N\lambda} = dt$$

Integrating

$$\int_0^N \frac{dN}{\phi\Sigma - N\lambda} = \int_0^t dt$$

$$-\frac{1}{\lambda} \ln [\phi\Sigma - N\lambda]_0^N = t$$

$$\ln \left[\frac{\phi\Sigma - N\lambda}{\phi\Sigma}\right] = -\lambda t$$

Thus:

$$\frac{\phi\Sigma - N\lambda}{\phi\Sigma} = e^{-\lambda t}$$

or:

$$N\lambda = \phi\Sigma(1 - e^{-\lambda t}) \tag{B.4}$$

But since $A = N\lambda$, activity is given by:

$$A = \phi\Sigma(1 - e^{-\lambda t}) \tag{B.5}$$

The saturated activity will be given by equation B.5 in the limit of infinite irradiation time:

$$A_0 = \phi\Sigma(1 - e^{-\lambda\infty}) = \phi\Sigma \tag{B.6}$$

Substituting (B.6) into (B.5):

$$A = A_0(1 - e^{-\lambda t}) \tag{B.7}$$

The time spent in the irradiation chamber is merely equal to the irradiation volume divided by the flow rate:

$$t_1 = \frac{V_1}{R} \tag{B.8}$$

Thus:

$$A_1 = A_0(1 - e^{-\frac{\lambda V_1}{R}}) \tag{B.9}$$

where A_1 is the activity at the exit of the irradiation chamber.

B.3 Activity Entering the Detector Chamber

The concentration of activity entering the detection chamber is the produced activity times a decay factor to account for decay while traveling to the detector chamber. The time of transit is V_2/R and the activity entering the detector chamber is given by:

$$A_2 = A_1 e^{-\frac{\lambda V_2}{R}} \qquad (B.10)$$

B.4 Activity in Detector Chamber

The detector count rate will be proportional to the activity in the detector chamber. The constant of proportionality is the detector efficiency. In the case of mixed flow, consider the following detector volume:

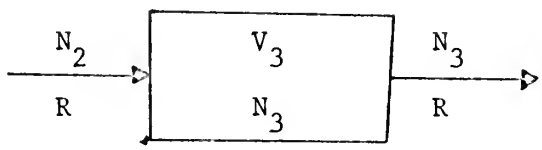

Perfect mixing demands that the concentration of N-16 in the chamber be uniform and equal to the exit concentration. Thus, the total number of atoms in the chamber will be N_3V_3, and the decay rate in the chamber will be λN_3V_3. This decay rate must be equal to the rate of atoms entering the chamber minus the rate exiting:

$$\lambda N_3V_3 = RN_2 - RN_3 \qquad (B.11)$$

Solving for N_3:

$$N_3(V_3\lambda + R) = RN_2$$

$$N_3 = \frac{RN_2}{R + V_3\lambda}$$

Multiplying by λ:

$$A_3 = \lambda N_3 = \frac{RA_2}{R + V_3\lambda}$$

Dividing numerator and denominator by R:

$$A_3 = \frac{A_2}{1 + \frac{\lambda V_3}{R}} \qquad (B.12)$$

Substituting B,7 and B,10 into B,12:

$$A_3 = A_0(1 - e^{-\frac{\lambda V_1}{R}})(e^{-\frac{\lambda V_2}{R}})(\frac{1}{1 + \frac{\lambda V_3}{R}}) \qquad (B.13)$$

The decay rate in the chamber is then A_3V_3 or:

$$DR \text{ mixed} = A_0(1 - e^{-\frac{\lambda V_1}{R}})(e^{-\frac{\lambda V_2}{R}})(\frac{V_3}{1 + \frac{\lambda V_3}{R}}) \qquad (B.14)$$

In the case of slug flow, consider the following detector volume:

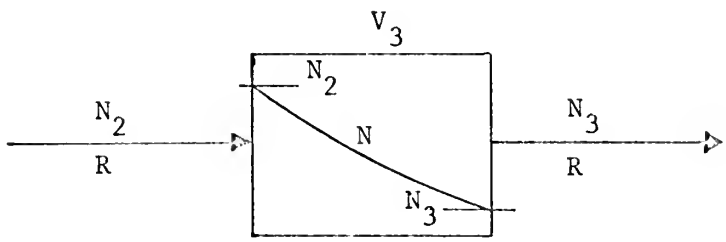

The concentration of N-16 in the chamber will follow an exponential decay along the length of the chamber such that:

$$N_3 = N_2 \, e^{-\frac{\lambda V}{R}}$$

where V varies from 0 to V_3 along the chamber. Again the decay rate in the chamber will equal the rate of entering minus the rate of exiting, or:

$$\text{DR slug} = RN_2 - RN_3$$

$$= RN_2\left(1 - e^{-\frac{\lambda V_2}{R}}\right)$$

$$\text{DR slug} = \frac{RA_2}{\lambda}\left(1 - e^{-\frac{\lambda V_3}{R}}\right) \qquad \text{(B.15)}$$

Substituting equations B.7 and B.10 into B.15:

$$\text{DR slug} = A_0\left(1 - e^{-\frac{\lambda V_1}{R}}\right)\left(e^{-\frac{\lambda V_2}{R}}\right)\left(\frac{R}{\lambda}\right)\left(1 - e^{-\frac{\lambda V_3}{R}}\right) \qquad \text{(B.16)}$$

APPENDIX C

N-16 FACILITY OPERATING PROCEDURE

C.1 Purpose

In order to facilitate the use of the present N-16 loop, the following "best operating procedure", resulting from the experience of the author, is set forth. Before attempting operation of the facility, however, the operator should read R. Mestemaker's thesis, Ref. 1, for additional background information, including many construction details.

C.2 Procedure

1. Load the in-pile section into the MIT Hohlraum, leaving a 12 inch length of the aluminum housing extending from the Hohlraum.

2. Connect the in-pile section to the out-of-pile section using the swagelok fittings provided. Note that the larger aluminum tube of the in-pile section is the inlet and the thinner tube the outlet.

3. Assemble the following pieces of electronic equipment and connect according to the schematic of Fig. 2.3.

High Voltage Power Supply - Cosmic Spectrastat 1001.

Linear Amplifier - Canberra Model 815.

Single Channel Analyzer - Canberra Model 830.

Scaler - Canberra Model 870.

Low Voltage Power Supply - Any 8^{V} DC source.

Timer - Any good timer.

Preamplifier - N-16 Loop Preamp.

Detector - 3 inch diameter NaI scintillator crystal and RCA photomultiplier tube.

4. Insert the detector (mounted on the preamp chassis) into the gun-barrel shield, running the attached cables through the access tube at the bottom. Cover the crystal with the annular water chamber.

5. Connect all tube fittings; open all valves (except the drain valve); energize the pump; and check for leaks.

6. Vent air from the detector chamber by removing the small screw from the top of the chamber. Reinsert the screw to seal the vent once all air has been bled from the chamber.

7. Energize the electronics and, after allowing three minutes for warm up, adjust to the following settings:

Low Voltage Supply: 8 volts.

High Voltage Supply: set dial to 7.00 ($\simeq$ 880^{V}).

Linear Amplifier: negative input, minimum gain.

Single Channel Analyzer: set base line at 9.00; set window to a near-closed position.

Scaler: "on".

Slowly increase the base line of the SCA until the scaler begins counting the MITR background peak at about 9.50 to 9.60. Having thus ascertained the correct operation of the detector and counting electronics, set the base line back to 9.00 and open the window to the wide-open position.

8. Place the lead detector chamber shield on top of the chamber to reduce the background.

9. Close the flow meter and the flow meter by-pass valve.

10. Open the lead and steel shutters to the Lattice Hohlraum to initiate irradiation of the in-pile section.

11. Set the scaler to the "gate" position and measure background at zero flow rate but with the pump motor energized.

12. Proceed with the experiment using Figure C.1 to convert flow meter readings to true flow rate. After changing the flow conditions, allow the system at least one minute to reach steady state before taking any measurements.

13. When completed, shut all valves, and de-energize the pump and electronics, being careful to slowly reduce the high voltage level before turning it off. Close the lead and steel shutters and allow the in-pile section sufficient time to "cool" before removing from the Hohlraum (about 12 hours).

C.3 Gas Purges

1. Connect the gas bottle to the purge line at the rear of the N-16 cart.

2. Close all valves in the purge line.

3. Crack the main gas bottle valve.

4. Crack the purge line check valve just downstream of the gas bottle.

5. Slowly open the purge valve at the rotameter-type gas flow

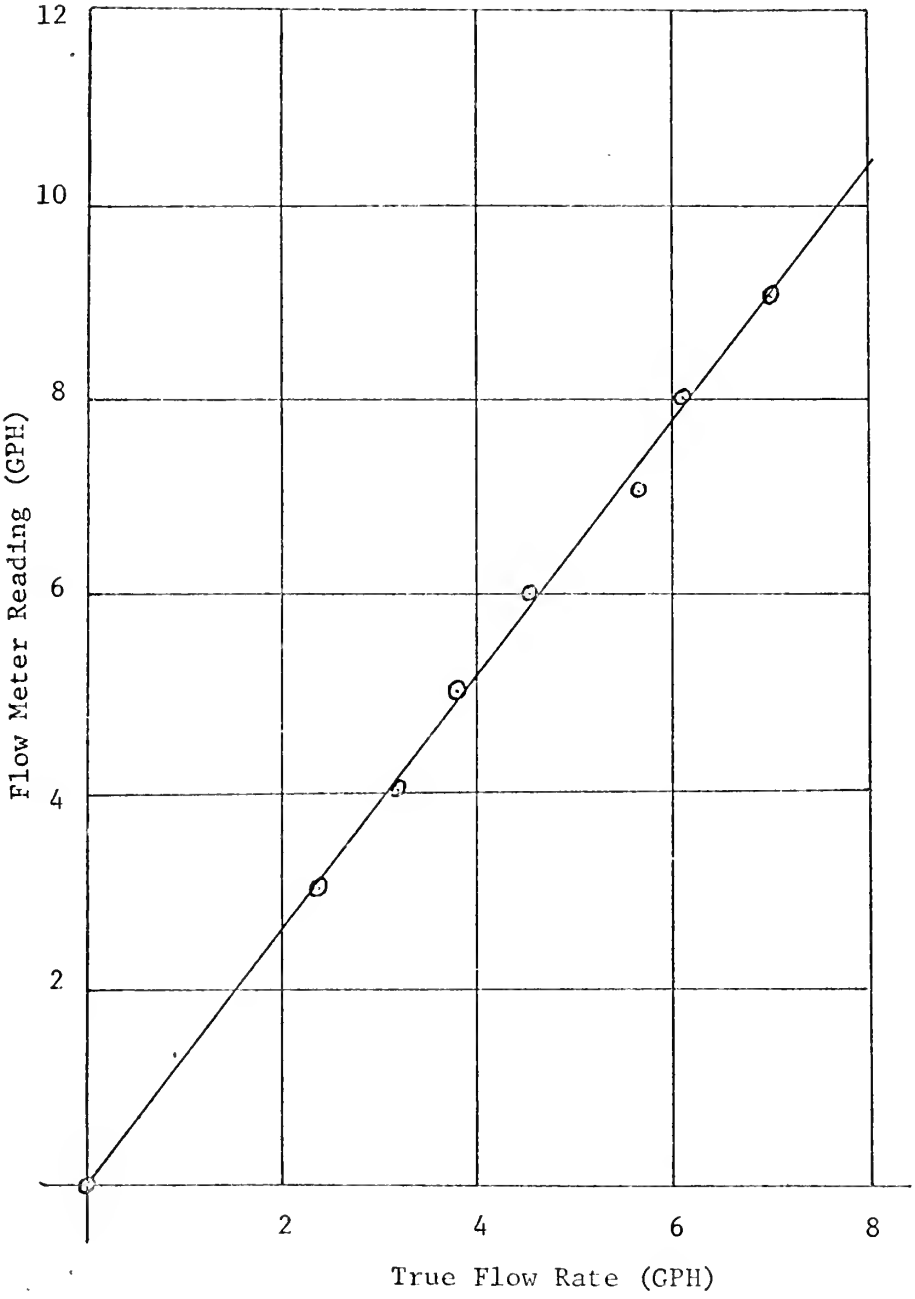

Figure C.1
Flow Meter Calibration

meter and adjust flow to about 2 cubic feet per hour.

6. Energize the pump and open all flow valves (except the drain valve) in order to obtain maximum flow rate.

7. Purge the system in this manner for about 15 minutes.

C.4 Chemical Additions

Chemicals should be added to the system at the purge tank. In the case of acid addition, only small amounts should be added at a time, and, after one minute, the pH measured by testing a sample taken at the drain valve.

C.5 Flushing the System

The system is most efficiently flushed by opening the drain valve completely at full flow rate. The level of water in the purge tank should be allowed to drop to within one inch of the bottom and then refilled with fresh water. This process should be continued until measurements indicate pure water at the drain valve.

APPENDIX D

SAMPLE CALCULATIONS

D.1 N-16 Removal

N-16 removal may be determined as follows:

D = % N-16 removed.

B = Background count rate (cpm).

N = Observed count rate (cpm).

M = True count rate = N - B (cpm).

N* = Reference activity = N for glass beads.

M* = N* - B = True reference activity.

Then $D = (1 - \frac{M}{M^*}) \times 100\%$.

Consider, for example, the following data taken on 4 April 1969 on the second ZrO_2 sample tested in the N-16 facility:

Background (measured before run): 32,158 counts in 2 min.

Flow Rate: 3.1 GPH

Counting Time: 2 min.

Glass Beads: 66,744 counts

ZrO_2 Sample: 51,822 counts

Background (measured after run): 32,654 counts in 2 min.

The value for background rate for this run is the average of the rates before and after the run.

$$B = 32,158 + 32,654 = \frac{64,812}{4 \text{ min.}} = 16,203 \text{ cpm.}$$

$$N^* = \frac{66,744 \text{ cpm}}{2} = 33,372 \text{ cpm.}$$

$$N_{ZrO_2} = \frac{51,822}{2} \text{ cpm} = 25,911 \text{ cpm.}$$

$$M^* = N^* - B = 33,372 - 16,203 = 17,169 \text{ cpm.}$$

$$M_{ZrO_2} = N - B = 25,911 - 16,203 = 9,708 \text{ cpm.}$$

$$\therefore \quad D_{ZrO_2} = \left(1 - \frac{9,708}{17,169}\right) \times 100\% = (1 - .565) \times 100\%.$$

Thus

$$D_{ZrO_2} = 43.5\%$$

D.2 Signal to Noise Ratio

Let Sn = signal to noise ratio

Then $Sn = \frac{\text{true count rate}}{\text{background count rate}} = \frac{M}{B}$

Consider the following data taken 17 February 1969:

Background: 66,602 cts in 5 min.

Flow Rate: Max. (> 7GPH)

Counting Time: 1 min.

Glass Beads: 72,790 counts.

$$\text{Thus } B = \frac{66,602 \text{ cts}}{5 \text{ min}} = 13,320 \text{ cpm}$$

$$N = 72,790$$

$$M = 72,790 - 13,320 = 59,470 \text{ cpm}$$

$$\therefore \quad Sn = \frac{59,470}{13,320} = 4.45$$

APPENDIX E

REFERENCES

1. Mestemaker, R.J., "Development and Test of a Facility to Study N^{16} Radiochemistry in Reactor Coolant Water", Master's Thesis, M.I.T., Department of Nuclear Engineering (February 1968).

2. Lauritsen, T., and Ajzenberg-Selove, F., "Energy Levels of Light Nuclei - May 1962", NRC 61-5, 6-223.

3. Scott, S.A., and Notea, A., "The Decay of N-16", Instrument Applications, (1965).

4. Driscoll, M.J., "The Removal of N-16 Activity from H_2O", 22.42 Project Report, M.I.T. Department of Nuclear Engineering (Fall 1962).

5. Forbes, I.A., "The Filtration of Nitrogen-16 From Water", 22.42 Project Report, M.I.T. Department of Nuclear Engineering (Spring 1966).

6. Coppola, E.J., "A Study of N^{16} Radiochemistry", 13.71 Project Report, MIT Department of Nuclear Engineering, (Summer 1968).

7. Fay, R.J., "Possible Detectors for the N^{16} Loop", 22.90 Project Report, MIT Department of Nuclear Engineering, (January 1969).

8. Massin, H.L., "Determination of the Efficiency for a Cerenkov Detector in the MITR Subcritical Lattice Facility", Master's Thesis, MIT Department of Nuclear Engineering, (August 1967).

9. Scott, S.A., and Notea, A., "Monitoring Reactor Power by N-17 Neutron Decay", American Nuclear Society Transactions, Volume 8, No. 1 (1965).

10. Scheiffer, J.J., and Adloff, J.P., "Formes Chemiques de L'Azote", Radiochimica Acta, 3, No. 3, 145 (1964).

11. Lewis, R.E., Butler, T.A. and Lamb, E., "An Aluminosilicate Ion Exchanger for Recovery and Transport of ^{137}Cs from Fission-Product Wastes", Nuclear Science and Engineering, 24, 118-122 (1960).

12. Amphlett, C.B., Inorganic Ion-Exchangers,(N.Y.: Elsevier Publishing Company, 1964).

13. Keen, N.J., "Studies on the Extraction of Uranium From Sea Water", The Journal of the British Nuclear Energy Society, Volume 7, No. 2, (April 1968).

14. Sweeton, F.H., and Baes, C.F., Jr., "Magnetite as a High-Temperature Adsorbent in Pressurized-Water Systems", American Nuclear Society Transactions, Volume 7, No. 1, (June 1964).

15. Michael, N., Sterling, R.F., and Cohen, P., "Inorganic Ion-Exchange Resins Could Purify Hotter Reactor Water", Nucleonics, Volume 21, No. 2, (February 1963).

16. Sherwood, T.K., and Pigford, R.L., Absorption and Extraction, 375-382, (New York: McGraw Hill Book Company, Inc., 1952).

17. Mittl, R.L., and Theys, M.H., "N^{16} Concentration in EBWR", Nucleonics, Volume 19, No. 3, (March 1961).

18. Whitham, G.K., and Smith, R.R., "Water Chemistry in a Direct-Cycle Boiling Water Reactor", Proceedings of the Second United Nations International Conference on the Peaceful Uses of Atomic Energy, Volume 7, (United Nations 1958).